Monitoring stray natural gas in groundwater with dissolved nitrogen. An example from Parker County, Texas

Toti E. Larson[1], Jean-Philippe Nicot[1], Patrick Mickler[1], M. Clara Castro[2], Roxana Darvari[1], Tao Wen[2,3], and Chris M. Hall[2]

[1]Bureau of Economic Geology, The University of Texas at Austin, Austin, TX, 78713, USA

[2]Department of Earth and Environmental Sciences, University of Michigan, Ann Arbor, MI, 48109, USA.

[3]Earth and Environmental Systems Institute, Penn State University, University Park, PA, 16802, USA.

Key Points:

- Using dissolved nitrogen in groundwater to monitor for infiltration of stray natural gas
- Using geochemical mixing models to differentiate gas- and aqueous-phase transport mechanisms in nature

Corresponding author: T. E. Larson, toti.larson@beg.utexas.edu

Abstract

Concern that hydraulic fracturing and natural gas production contaminates groundwater requires techniques to attribute and estimate methane flux. Although dissolved alkane and noble gas chemistry may distinguish thermogenic and microbial methane, low solubility and concentration of methane in atmosphere-equilibrated groundwater precludes the use of methane to differentiate locations affected by high- and low-flux of stray methane. We present a method to estimate stray gas infiltration into groundwater using dissolved nitrogen. Due to the high concentration of nitrogen in atmospheric-recharged groundwater and low concentration in natural gas, dissolved nitrogen in groundwater is much less sensitive to change than dissolved methane and may differentiate groundwater affected high- and low-flux of stray natural gas. We report alkane and nitrogen chemistry from shallow groundwater wells and 8 natural gas production wells in the Barnett Shale footprint to attribute methane and estimate mixing ratios of thermogenic natural gas to groundwater. Most groundwater wells have trace to non-detect concentrations of methane. A cluster of groundwater wells have greater than 10 mg/L dissolved methane concentrations with alkane chemistries similar to natural gas from the Barnett Shale and/or shallower Strawn Group suggesting that localized migration of natural gas occurred. Two-component mixing models constructed with dissolved nitrogen concentrations and isotope values identify three wells that were likely affected by a large influx of natural gas with gas:water mixing ratios approaching 1:5. Most groundwater wells, even those with greater than 10 mg/L methane, have dissolved nitrogen chemistry typical of atmosphere equilibrated groundwater suggesting natural gas:water mixing ratios smaller than 1:20.

1 Introduction

Unconventional natural gas extraction occurs near municipalities including the Dallas – Fort Worth metroplex and this has increased public awareness about the potential for groundwater contamination associated with hydraulic fracturing. Horizontal drilling and hydraulic fracturing technologies are used to increase permeability in shale and tight formations. There is concern that hydraulic fracturing will cause natural gas, reservoir brines and associated hydraulic fracturing fluids to migrate from natural gas reservoirs to shallower groundwater aquifers (< 250m depth) thereby threatening drinking water supplies [*Osborn et al.*, 2011; *Jackson et al.*, 2013; *Thompson*, 2012; *Christian et al.*, 2016]. Geochemical studies in the Marcellus Shale of Pennsylvania, the Utica Shale of New York

state, and the Barnett Shale, Eagle Ford Shale and Haynesville Shale of Texas have attributed methane in shallow groundwater to either deep thermogenic 'stray' or shallow low-temperature microbial sources [*Molofsky et al.*, 2013; *Siegel et al.*, 2015; *Osborn et al.*, 2011; *Jackson et al.*, 2013; *Darrah et al.*, 2014; *Christian et al.*, 2016; *Wen et al.*, 2016, 2015; *Nicot et al.*, 2017]. Here, the phrase 'stray gas' refers to natural gas, of an undetermined origin, that is encountered unexpectedly in shallow groundwater aquifers. Source attribution techniques for stray gas commonly employ concentration ratios of methane, ethane and propane and their stable carbon and hydrogen isotope ratios (i.e., Bernard and Schoell plots) [*Rostron and Arkadakskiy*, 2014; *Whiticar*, 1999; *Grossman et al.*, 1989; *Prinzhofer et al.*, 2000; *Bernard et al.*, 1977; *Schoell*, 1980]. Bernard and Schoell plots can effectively differentiate microbial and thermogenic sources of methane because low temperature methanogenesis generates methane with a carbon isotope value that is lower than methane derived from thermogenic processes, and thermogenic natural gas typically contains appreciable amounts of ethane and propane [*Prinzhofer et al.*, 2000; *Grossman et al.*, 1989; *Bernard et al.*, 1977; *Schoell*, 1980]. Attribution with alkane chemistry is complicated by the potential for mixing of multiple sources of thermogenic natural gas of different maturity with additional sources of microbial methane [*Moritz et al.*, 2015; *Zhang et al.*, 1998]. In addition to mixing of multiple sources, anaerobic methane oxidation is a common groundwater process that can modify the carbon isotope values and relative concentrations of residual dissolved alkanes [*Zhang et al.*, 1998; *Barker and Fritz*, 1981] and dissolved inorganic carbon (DIC) [*Zhang et al.*, 1998; *Grossman et al.*, 1989; *Barker and Fritz*, 1981]. To a lesser degree, carbon isotope values of methane and alkane ratios may be affected by transport and migration, but these effects are likely small [*Fuex*, 1980; *Prinzhofer et al.*, 2000; *Lu et al.*, 2015]. For these reasons, additional geochemical tools including dissolved noble gases, which can provide further insight into methane source attribution and identify possible transport mechanisms of stray gas, has been applied to natural gas migration studies.

Dissolved noble gas concentrations and their isotope ratios are used to estimate groundwater recharge temperatures [*Solomon et al.*, 1996] and to trace crustal fluid processes such as gas-phase transport through water saturated media [*Ballentine et al.*, 2002; *Gilfillan et al.*, 2009; *Darrah et al.*, 2014; *Wen et al.*, 2016]. These efforts take advantage of differences in crustal, mantle and atmosphere noble gas concentrations and isotope ratios along with the inert behavior of noble gases, which are largely unaffected by subse-

78　　quent microbial processes and reaction with geologic substrate [*Ballentine et al.*, 2002].

79　　*Ballentine et al.* [2002] establishes the fundamental relationships that govern noble gas

80　　fractionation during single- and two-phase transport, with a specific focus on solubility ef-

81　　fects. Related to natural gas transport, exchange or fractionation of gases between gas- and

82　　aqueous-phases occurs when a stray gas phase comes into contact with an aqueous phase.

83　　Exchange of chemical components between the gas and aqueous phase may add 'excess'

84　　or remove 'strip' dissolved gases from groundwater depending on the degree of gas-water

85　　interaction, concentration gradients, temperature, and Henry's Law constants [*Ballentine

86　　et al.*, 2002; *Cey et al.*, 2009]. Three studies report dissolved noble gas isotopes to evaluate

87　　elevated natural gas in shallow groundwater wells from the Barnett Shale of Texas [*Dar-

88　　rah et al.*, 2014; *Wen et al.*, 2016, 2017] and the Marcellus Shale of Pennsylvania [*Darrah

89　　et al.*, 2014]. Within the Barnett Shale, these studies identify a spatial cluster of ground-

90　　water wells that contain high concentrations of natural gas and conclude that the natural

91　　gas is likely sourced from the Strawn Group that is stratigraphically above the Barnett

92　　Shale, which is the target of hydraulic fracturing [*Darrah et al.*, 2014; *Wen et al.*, 2016,

93　　2017]. *Nicot et al.* [2017] sampled an extensive region of the Barnett Shale footprint (509

94　　groundwater wells covering 14,500 km^2) to assess the extent of this spatial cluster and to

95　　evaluate likely sources of the stray natural gas. The cluster of groundwater wells with el-

96　　evated dissolved methane concentrations is located near the Parker and Hood County line

97　　and these wells have high concentrations of dissolved methane and lower than expected

98　　concentrations of nitrogen, ^{20}Ne, ^{36}Ar, and ^{84}Kr for atmosphere-equilibrated groundwater

99　　[*Darrah et al.*, 2014]. From this same cluster of groundwater wells *Wen et al.* [2016] re-

100　　port a positive correlation between dissolved methane and ^{4}He, ^{21}Ne, and ^{40}Ar concentra-

101　　tions, noble gas isotopes which are enriched in the crust relative to the atmosphere [*Bal-

102　　lentine et al.*, 2002]. Citing a poor correlation between chloride and dissolved methane in

103　　groundwater wells, *Darrah et al.* [2014] suggest that thermogenic hydrocarbon gas migra-

104　　tion was not accompanied by brine and therefore not transported within an aqueous phase.

105　　Rather, thermogenic gas in the shallow groundwater was likely transported as a free-gas

106　　phase. *Wen et al.* [2016] directly compares ^{4}He/^{20}Ne ratios of dissolved gas in ground-

107　　water samples to natural gas samples collected from the Strawn Group and concludes that

108　　stray gas in these water wells is most likely sourced from the Strawn Group, a conclu-

109　　sion that was also reached by *Darrah et al.* [2014]. Although these studies agree on the

110　　source of the thermogenic methane, they come to different conclusions on the transport

111   mechanism of natural gas from the Strawn Group to the shallow groundwater of the Trin-

112   ity Formation; *Darrah et al.* [2014] suggests transport along well annulus associated with

113   poor cementing techniques, whereas *Wen et al.* [2016] suggests transport through natural

114   pathways and hydrologic contacts between the overlying Trinity Aquifer and underlying

115   natural gas reservoirs in the Strawn Group. *Nicot et al.* [2017] provides geologic context to

116   conclude that the vertical distance from the groundwater well screen to the unconformable

117   contact between the Trinity Formation the Strawn Group is a more important factor than

118   distance to Barnett Shale and conventional horizontal wells. These observations are used

119   to show that, at least within the Barnett Shale footprint, hydraulic fracturing of the Bar-

120   nett Shale has not provided the source or transport mechanism for natural gas observed in

121   shallow groundwater [*Darrah et al.*, 2014; *Wen et al.*, 2016; *Nicot et al.*, 2017].

122   Nitrogen is the most abundant non-hydrocarbon gas associated with natural gas

123   reservoirs [*Ballentine et al.*, 2002; *Krooss et al.*, 1995] with measured concentrations that

124   range from trace to nearly 100 percent [*Mingram et al.*, 2003; *Krooss et al.*, 1995; *Márquez

125   et al.*, 2013; *Ballentine et al.*, 2002; *Jenden et al.*, 1988]. Subsurface sources of nitrogen

126   gas include metamorphic and diagenetic alteration of high ammonium clays, primordial

127   gas from the mantle, denitrification of nitrate, and thermogenic cracking of sedimentary

128   organic matter [*Krooss et al.*, 1995; *Golding et al.*, 2013; *Jenden et al.*, 1988]. The dom-

129   inant source of dissolved nitrogen in shallow groundwater is atmospheric in origin and

130   incorporated during equilibrium dissolution in the near surface (δ^{15}N=+0.7‰) [*Klots and

131   Benson*, 1963] and as an excess gas trapped as bubbles of air (δ^{15}N=0‰) [*Vogel et al.*,

132   1981; *Heaton and Vogel*, 1981; *Cey et al.*, 2009]. At groundwater recharge temperatures

133   of $18-20°$C dissolved nitrogen concentrations of $14-15$ mg/L are expected for atmo-

134   spheric saturated water (ASW) based on Henry's law calculations [*Weiss*, 1970]. Unlike

135   noble gases that are unaffected by microbial processes and are inert with respect to re-

136   action with geologic substrate, the nitrogen cycle in groundwater is more complex and

137   additional processes that affect nitrogen must be considered. Foremost, microbial denitri-

138   fication of nitrate produces nitrogen gas which can affect the dissolved nitrogen concen-

139   tration and its δ^{15}N value [*Knowles*, 1982]. Important to methane studies, stray natural

140   gas will increase the availability of methane and may activate anaerobic oxidation cou-

141   pled to nitrate [*Knowles*, 1982; *Ettwig et al.*, 2010] and/or sulfate [*Valentine and Reeburgh*,

142   2000] reduction. In reducing groundwater systems, denitrification of nitrate to nitrogen is

143   thermodynamically favored over sulfate reduction [*Stumm and Morgan*, 2012], and in both

144 instances the oxidized by-product of methane is CO_2 in the form of dissolved inorganic

145 carbon (DIC). Studies addressing dissolved nitrogen must therefore account for dissolved

146 nitrogen, methane, and inorganic carbonate species.

147 This study tests the hypothesis that dissolved nitrogen chemistry may provide an ad-

148 ditional means to distinguish sources of stray gas and help differentiate regions with high-

149 and low-flux of stray gas. This hypothesis is based on stray gas having a nitrogen concen-

150 tration that is lower than atmospheric, and a nitrogen isotope value that is distinct from

151 atmospheric such that the residual reservoir of dissolved nitrogen in the groundwater phase

152 will be lower than expected for ASW (i.e., 'stripping' of dissolved nitrogen) and isotopi-

153 cally distinct (i.e., 'isotope exchange'). In this study we use dissolved gas chemistry from

154 samples collected within the Barnett Shale footprint. Measured concentrations of dissolved

155 methane are used as a primary means to identify groundwater wells that are potentially

156 affected by stray gas. Dissolved alkane chemistry is used to attribute methane to either

157 microbial or thermogenic sources. Mixing models based on the relationships presented

158 by *Ballentine et al.* [2002] are constructed for dissolved nitrogen concentration and its

159 $\delta^{15}N$ value with consideration given to the addition of dissolved nitrogen through anaer-

160 obic methane oxidation. This research builds off published observations and conclusions

161 [*Darrah et al.*, 2014; *Wen et al.*, 2016, 2017] for shallow groundwater wells in the Bar-

162 nett Shale footprint. Comparing dissolved nitrogen chemistry results reported here with

163 dissolved noble gas ratios measured from the same wells [*Wen et al.*, 2016] and from the

164 same geographic cluster of wells as reported by *Darrah et al.* [2014] provides a unique

165 means to test our hypothesis. We specifically chose the nitrogen system to develop gas

166 mixing models rather than using the alkane system alone because of the contrasting sen-

167 sitivity to change between these systems. Whereas the migration of small volumes of

168 stray natural gas into ASW will have large effects on observed dissolved methane con-

169 centrations, larger volumes of natural gas are required to change the dissolved nitrogen

170 concentration of ASW, and even more volumes are required to change the $\delta^{15}N$ value of

171 ASW. Therefore, nitrogen, along with noble gas ratios, may provide an important means

172 to estimate the amount of stray natural gas that has infiltrated into a shallow groundwater

173 aquifer.

2 Study area

The study area is within Parker and Hood Counties in north central Texas, just west of the Dallas-Fort Worth Metroplex (Fig. 1). Depths to the top of the Barnett Shale approach 1600 to 1700 meters near the Parker-Hood County line [*Pollastro et al.*, 2007]. The Barnett Shale is Mississippian in age and is the target formation for unconventional natural gas hydraulic fracturing with over 20,000 natural gas production wells drilled as of 2015 [*Pollastro et al.*, 2007; *Jarvie et al.*, 2007; *IHS*, 2015]. Natural gas within the Barnett Shale is thermogenic in origin [*Montgomery et al.*, 2005] and is the primary source of natural gas and oil in the Fort Worth Basin, supplying conventional reservoirs within the Ellenburger of Ordovician age, the Marble Falls and the Strawn of Pennsylvanian age, and other rock units [*Jarvie et al.*, 2007; *Montgomery et al.*, 2005; *Loucks and Ruppel*, 2007]. Syn- and post-depositional burial depths were sufficient to reach oil- and gas-generation stages, and within the study area the Barnett Shale generated significant volumes of natural gas through multi-stage thermal cracking of kerogen, bitumen and oil [*Montgomery et al.*, 2005; *Jarvie et al.*, 2007; *Pollastro et al.*, 2007]. Transport of natural gas from the Barnett Shale into surrounding reservoirs likely occurred during gas-generation stages as increased thermal maturity resulted in pressure increases and microfracturing, thereby creating pathways for subsurface fluid migration [*Jarvie et al.*, 2007; *Wen et al.*, 2017]. The Barnett Shale is uncomformably overlain by the Pennsylvanian-aged Marble Falls Limestone which is a massive limestone unit. Above the Marble Falls Limestone, and of primary importance to this study, is the Pennsylvanian-aged Strawn Group which consists of fluvial-deltaic sandstone facies that have trapped migrating oil and gas from source rocks that may include the underlying Mississippian Barnett Shale, coeval organic-rich Pennsylvanian rocks, or the Late Devonian Woodford shale [*Ball and Perry*, 1995; *Brown*, 1973]. The isolated and discontinuous nature of natural gas pockets within the Strawn Group have made it a difficult reservoir to target for natural gas production, however its potential as a natural reservoir has been explored since the 1930's.

Unconformably above the Strawn Group in the study area lies early Cretaceous sandstone, basal conglomerates and interbedded clays that are referred to as the Trinity Group. The Trinity Group hosts the Trinity aquifer, which is the primary fresh water source for the study area [*Ashworth et al.*, 1995; *Chaudhuri and Ale*, 2013] and the primary aquifer from which groundwater samples were collected in this study. The unconformable contact between the underlying Strawn Group and the Trinity Group does provide for a hydrologic

207   connectivity. Recharge to the Trinity Aquifer occurs through precipitation on exposed out-

208   crop and downward seepage from rivers. Recharge rates within the Trinity Aquifer be-

209   tween 2-3 centimeters per year are reported [*Nordstrom*, 1982], however this is an average

210   for a large region and may not be representative of recharge rates within the field area.

3 Methods

3.1 Groundwater collection

213   Groundwater samples were collected from residential, irrigation, and municipal

214   groundwater wells between December 2013 and January 2015 with a specific focus on

215   Parker and Hood Counties (Fig. 1). Samples collected for dissolved gases, dissolved in-

216   organic carbon, sulfate, and nitrate were collected at the same time at each well. Noble

217   gas data from *Wen et al.* [2016] that are discussed in this paper were also collected at

218   the same time. Sample locations cover a wide geographical area that has seen consider-

219   able activity from hydraulic fracturing operations [*Nicot et al.*, 2014]. Groundwater wells

220   in this area (depths < 250 meters) are typically sourced in the lower Cretaceous Trinity

221   aquifer system [*Nicot et al.*, 2014; *Nicot*, 2013]. However, some groundwater wells pene-

222   trate the unconformably underlying Strawn Group. Water samples were collected for dis-

223   solved methane, ethane, propane and nitrogen concentration and stable isotope measure-

224   ments. Additional water samples were collected to measure dissolved inorganic carbon

225   (DIC) concentrations and carbon isotope measurements, and sulfate and nitrate concen-

226   trations. Specific requirements were followed to obtain representative groundwater sam-

227   ples. We ensured that sampled groundwater wells were (1) drilled to shallow groundwater

228   aquifers and (2) did not contain any type of storage reservoir or filtration device.

229   Groundwater wells were allowed to flow for at least fifteen minutes to purge stand-

230   ing water, remove any pockets of air that may have accumulated through time and un-

231   til pH, temperature and ORP stabilized. Water samples for dissolved gas analysis were

232   collected using a flow-through serum bottle sampling technique with 80ml glass serum

233   vials capped with 20mm blue chlorobutylm septa (Bellco part number 2048−11800) and

234   crimped with an aluminum seal. The vials are septa sealed prior to filling with water and

235   two syringes (one fill and one back-vent syringe) are used to fill the vial with groundwa-

236   ter using a small length of clear tubing. At least five vial volumes of water are flushed

237   through the vial. This procedure of pre−capping, filling and flushing the vials is essential

238 to ensure that dissolved gas is not lost during sampling, residual gas bubbles are purged,

239 and to minimize the potential for atmospheric contamination. This flow-through sampling

240 technique also has the added benefit that excess dissolved gas (i.e., gas bubbles formed in

241 the groundwater well) is not collected. Water samples collected in the serum bottles are

242 stored at 4°C and acidified with 0.1 ml of 12M hydrochloric acid. Groundwater samples

243 for DIC measurement were filtered with a 0.2 micron filter, collected in 40ml amber vials

244 without headspace, and refrigerated until analysis.

3.2 Groundwater analysis

246 Dissolved gas concentrations and carbon isotope values are measured for each sam-

247 ple using a headspace equilibration technique [*Kampbell and Vandegrift*, 1998]. A headspace

248 of pure helium is created in the serum vial by simultaneously injecting 5ml of pure he-

249 lium while removing 5ml of water using two Hamilton Gastight series 1000 headspace

250 syringes. Once completed both syringes are simultaneously removed and the serum bot-

251 tle is preserved for subsequent analysis. To screen all samples, 4ml of the removed water

252 is immediately injected into a 6ml Labco Exetainer headspace vial that was pre-purged

253 with helium and evacuated. Adding this volume of water to the Exetainer in no way af-

254 fects the integrity of the sample in the serum vial, but allows us to automatically screen

255 a large number of samples for dissolved methane concentration. Samples without de-

256 tectable concentrations of methane are not reanalyzed routinely (however a subset of non-

257 detect samples were reanalyzed for assurance purposes), whereas samples with detectable

258 methane are re-analyzed directly from the serum bottle using a manually operated syringe.

259 The automated screening technique is simply a means to identify samples that are free of

260 methane, which are not reanalyzed using the more labor intensive manual serum bottle

261 analysis technique.

262 Concentrations of alkanes (C1 through C3) are measured using an Agilent 7890 gas

263 chromatograph optimized for natural gas with a poraplot Q column and a Flame Ionization

264 Detector (FID). A series of six internal methane gas standards that range from 200ppb

265 to 7.5%, Scott Gas natural gas standard (TNB00060-14) for methane (88.73%), ethane

266 (3.5%), and propane (1.0%), and Scott Gas natural gas mixture for methane (100ppm),

267 ethane (100ppm) and propane (100ppm) were used for calibration. Exactly 225 micro-

268 liters of headspace gas is injected, yielding an analytical detection limit of approximately

269 500ppb for methane, ethane and propane. Measured headspace concentrations of methane,

9

270 ethane, propane and nitrogen are used to calculate dissolved gas concentrations [*Kamp-*

271 *bell and Vandegrift*, 1998]. These calculations account for the volume of liquid and gas

272 headspace in the serum bottle, temperature, and Henry's Law constants for each gas species.

273 Detection limits of at least 0.001 mg/L for methane (C1), 0.002 mg/L for ethane (C2),

274 and 0.003 mg/L for propane (C3) are achieved [*Kampbell and Vandegrift*, 1998]. Less

275 than 0.5% analytical error is routinely achieved on standard reference gases. Replicate

276 analyses of dissolved gas samples, which combines errors associated with sample prepara-

277 tion and analysis were less than 4%. In terms of error of dissolved methane concentration,

278 a 4% total error correlates to an uncertainty of $\pm$ 0.05 mg/L for a sample with a 1.0 mg/L

279 concentration of dissolved methane and $\pm$ 0.5 mg/L for a sample with 8.0 mg/L dissolved

280 methane, for example.

281   Dissolved nitrogen concentrations and nitrogen isotope values were measured using

282 a 225 microliter injection of headspace gas that was also used to measure carbon isotopes

283 of methane. Here, we used an Agilent 7890 GC with a 5 mol sieve column and a non-

284 destructive Thermal Conductivity Detector (TCD). This method provided excellent sep-

285 aration of nitrogen, oxygen, and methane, which is critical for accurate methane carbon

286 isotope analysis; any tailing of the nitrogen peak over the methane peak may cause errors

287 during carbon isotope measurement due to formation of N_2O in the ion source, the degree

288 of which will depend on the relative concentrations of methane and nitrogen. Nitrogen

289 concentrations were measured using peak areas collected on the TCD and were calibrated

290 against a series of five internally developed nitrogen standards and a 2.5 % nitrogen in

291 natural gas standard (Supelco cat. no. 303101). Methane is combusted to CO_2 using a

292 narrow-bore quartz glass reactor heated to 700°C packed with copper oxide and analyzed

293 for its $\delta^{13}C$ value using a Thermo Fisher Scientific Delta V Isotope Ratio Mass Spectrom-

294 eter directly coupled to the GC-TCD through a Conflo IV peripheral. Carbon isotopes

295 are calibrated against measurements of three internal methane standards ($\delta^{13}C$ =-52.8, -

296 39.8, and -95.5‰) that are calibrated with respect to NBS-19 having a $\delta^{13}C_{VPDB}$ equal to

297 +1.95‰. The $\delta^{13}C$ value of these three internally developed methane standards were ver-

298 ified by sending aliquots of gas for measurement at Isotech Laboratories. Dissolved nitro-

299 gen isotope values are measured directly on N_2 gas using a Thermo Fisher Scientific Delta

300 V Isotope Ratio Mass Spectrometer directly coupled to the GC-TCD through a Conflo IV

301 peripheral. Nitrogen isotope values are reported with respect to $\delta^{15}N_{AIR}=0‰$ using an

302 air reference gas and a natural gas standard with 2.5% nitrogen. Replicate analyses of dis-

solved methane samples resulted in a standard deviation of ±0.35% for δ^{13}C for methane

and ±0.4% for δ^{15}N for nitrogen.

Dissolved inorganic carbon (DIC) concentrations and carbon isotope values were

measured using a Thermo Electron Gas Bench II coupled to a Thermo Electron MAT

253 Isotope Ratio Mass Spectrometer (IRMS) [*Torres et al.*, 2005; *Waldron et al.*, 2014].

All DIC δ^{13}C values are reported relative to NBS-19 having a δ^{13}C$_{PDB}$ equal to +1.95‰

with a standard deviation of ± 0.15‰. DIC concentrations were calculated using a series

of six internal calibration standards that cover the range of concentration measured. An

error of less than 3% was achieved for all concentration measurements.

4 Results

4.1 Produced gas chemistry

Samples of natural gas were collected from nine producing wells (8 from the Barnett

Shale and 1 from the Strawn Group and analyzed for their natural gas chemistry. Loca-

tions of the sampled producing wells are illustrated in Fig. 1. We include published data

from *Darrah et al.* [2014] for Strawn and Barnett production wells in addition to produc-

tion wells collected in this study. Alkane and nitrogen concentrations and the stable car-

bon isotope ratios of methane and nitrogen are listed in Table 1. Gas dryness (C1/C2+C3

alkane ratios) is plotted with respect to carbon isotope values of methane in Fig. 2. Gas

dryness averages 4.5 ± 0.8% (n=10) for the Barnett Shale and 9.9 ± 2.0% (n=5) for the

Strawn Group. Carbon isotope values of methane from the Barnett Shale and the Strawn

Group are indistinguishable at -47.2 ± 1.6‰ and -47.8 ± 0.5‰, respectively. These values

are consistent with those reported by *Rodriguez and Philp* [2010] for samples collected in

Parker county. Nitrogen molar concentrations of 0.9 ± 0.2% (n=10) and δ^{15}N values that

range from -1.8 to -7‰ (n=8) are measured for the Barnett Shale samples (Table 1). One

sample measured in this study area from the Strawn Group has a δ^{15}N value of -6.5‰ and

five samples from the Strawn Group have nitrogen molar concentrations that range from

2.7 to 5.6% (average = 3.94± 1.2% Table 1). Nitrogen concentrations measured in this

study are consistent with published nitrogen concentrations of 1.05 ± 0.2% (n=2) and 4.25

± 1.1% (n=4) measured from the Barnett Shale and Strawn Group, respectively [*Darrah

et al.*, 2014] (Table 1). In the following sections we develop a model to compare the ef-

fects of mixing groundwater water with low- and high-nitrogen natural gas representative

334 of nitrogen concentrations measured from the Strawn Group and Barnett Shale and dis-

335 cuss the effect that nitrogen content may have on resulting groundwater dissolved nitrogen

336 isotope values [*Kreitler and Browning*, 1983; *Kornacki and McCaffrey*, 2014].

337 ### 4.2 Spatial distribution of dissolved methane

338 Dissolved methane concentrations measured from 457 wells in Parker, Hood, Somervell

339 and surrounding counties are illustrated in Fig. 1. These data are reported in Table S2. of

340 *Nicot et al.* [2017]. Locations of hydraulic fracturing wells within these counties are also

341 illustrated. Dissolved methane concentrations are grouped using a modified classification

342 system outlined by the United States Department of the Interior Office of Surface Mining

343 [*Eltschlager et al.*, 2001]: < 0.1 mg/L 'trace'; 0.1 to 2 mg/L 'low'; 2-10 mg/L 'interme-

344 diate'; 10-28 mg/L 'high'; and > 28 mg/L 'elevated'. Using this classification, 424 out of

345 457 groundwater wells analyzed in this study yielded trace to low concentrations of dis-

346 solved methane [*Nicot et al.*, 2017]. Three clusters of samples with intermediate, high, and

347 elevated dissolved methane concentrations are identified (Fig. 1). The largest cluster is lo-

348 cated at the border of Parker and Hood counties (referred to as the 'Parker-Hood cluster').

349 Two smaller clusters are observed to the north 'North Parker cluster' and south 'Somervell

350 cluster' of the Parker-Hood cluster. Additional groundwater wells from the Parker-Hood

351 cluster were obtained to better delineate the spatial extent of this cluster. Here, we focus

352 on samples collected within and near the described clusters that come from 77 unique

353 groundwater wells for a total number of 118 samples with replicates. Comparison of dis-

354 solved methane concentrations from groundwater wells that were visited and sampled mul-

355 tiple times are in good agreement. More variability is observed for higher concentration

356 samples compared to wells with low to trace concentrations of dissolved methane. For

357 example, methane concentrations from repeat sampling of well BS200 are 24.5 and 18.3

358 mg/L, and 14.6 and 18.0 mg/L for well BS358. This observed variability with higher

359 concentration samples (i.e., > 20mg/L) is consistent with sampling effects observed by

360 [*Molofsky et al.*, 2016] for wells with high concentrations of dissolved methane and subse-

361 quent two-phase systems.

362 ### 4.3 Dissolved alkane chemistry

363 Methane, ethane, and propane concentrations, corresponding $\delta^{13}C_{methane}$ values,

364 and gas dryness (C1/(C2+C3) alkane ratios) are listed in Table 2. Gas dryness is plotted

with respect to carbon isotope values of dissolved methane in figure 2. Minimum concentration of methane for $\delta^{13}C_{methane}$ analysis is approximately 0.1 mg/L (compared to analytical detection limits of 0.001 mg/L for methane concentration); however most samples plotted have concentrations greater than 0.5 mg/L. Therefore, these data represent a subset (n=84) of samples collected in the field area, with most samples coming from the North Parker, Parker-Hood and Sommervell clusters. The North Parker cluster (five samples from two groundwater wells) contain low to intermediate methane concentrations (0.70 to 3.40 mg/L). Samples from the North Parker cluster preserve alkane chemistry results that are more similar to a microbial methane signature compared to other samples measured in this study. For example, groundwater well BS031 (n=3) has methane concentrations between 3.4 and 2.0 mg/L, non-detect concentrations of ethane and propane, and $\delta^{13}C_{methane}$ values between -62 and -67‰(Fig. 2). Two samples from groundwater well BS029 have higher $\delta^{13}C_{methane}$ values of -57 and -51‰, but non-detect concentrations of ethane and propane and a lower concentration of dissolved methane 0.7 and 1.0 mg/L. Eight additional samples taken within 10km of these two groundwater wells have trace (<0.1 mg/L) dissolved methane concentrations pointing to a localized nature for the intermediate dissolved methane concentrations in this area.

Further to the south, the Parker-Hood cluster (Fig. 1) is delineated by 47 groundwater wells that encompass an area of approximately 50km^2. $\delta^{13}C_{methane}$ values for samples from these groundwater wells range between -41 and -52‰, which is similar to $\delta^{13}C_{methane}$ values measured for methane from produced gas from the Barnett Shale and Strawn Group ($\delta^{13}C$ between -42 and -47‰; samples collected in this and other studies [*Rodriguez and Philp*, 2010]). Alkane ratios (C1/(C2+C3)) range from 3.3 to 22.7, which also closely matches alkane ratios from production wells for the Barnett Shale and Strawn Group collected within 10km of the Parker-Hood cluster (Fig. 2). The majority of the groundwater wells have dissolved methane concentrations above 2 mg/L, with nine groundwater wells having dissolved methane concentrations greater than 10 mg/L, and a maximum dissolved methane concentration of 31 mg/L (BS199) was measured. One groundwater well (BS555, well depth 95m) has vented natural gas since it was drilled in December, 2012. We measured a gas flow rate of 3L/minute at the head of this groundwater well and its alkane chemistry closely matches natural gas from the Barnett Shale and Strawn Group. Although groundwater wells BS199 and BS555 contain elevated and high dissolved methane concentrations > 20mg/L with a thermogenic signature that is

similar to natural gas from the Barnett Shale and Strawn Formation, a groundwater well within 100m of BS555 (BS544, well depth 125m) has a lower dissolved methane concentration of 2.6 mg/L. Methane at BS544 also has a thermogenic signature, but the measured difference in concentration over a short distance demonstrates the heterogeneity and localized nature of elevated dissolved methane concentrations in the Parker-Hood cluster. Six groundwater samples from the Parker-Hood cluster have low dissolved methane concentrations (0.16 to 0.84 mg/L) and methane $\delta^{13}C_{methane}$ values that are greater than the rest of the samples ($\delta^{13}C$ > -37‰). The wide range of carbon isotope values and alkane dryness in the measured groundwater samples relative to the more constrained range of values observed for produced natural gas from the Barnett Shale and Strawn Group is discussed in the following sections.

The Somervell cluster is 25 kilometers to the south of the Parker-Hood cluster (Fig. 1). Three different groundwater wells (8 samples) have dissolved methane concentrations that range from 0.64 to 11.3 mg/L. Similar to the Parker-Hood cluster, the highest concentration sample is within 500 meters of two groundwater wells with trace concentrations of dissolved methane, further suggesting the localized nature of the clusters defined by high dissolved methane concentration. Samples from the Somervell cluster show the greatest variability of $\delta^{13}C_{methane}$ and C1/(C2+C3) ratios, suggesting thermogenic and microbial methane source mixing (Fig. 2). Sample BS402 is unique in this dataset in that the dissolved methane has a $\delta^{13}C$ value of -79.6‰ suggesting formation from a CO_2 reduction methanogenic pathway [*Wolin and Miller*, 1987; *Whiticar*, 1999; *Zhang et al.*, 1998]. This is distinct from sample BS031 from the North Parker Cluster which is also microbial in nature, but more consistent with methane acetate methanogenesis.

4.4 Anaerobic methane oxidation

Measured concentration and carbon isotope values of dissolved inorganic carbon (DIC) range from 6.7 to 13.0 mmol/L with corresponding $\delta^{13}C$ values that range from -1.5 to -14‰ (n=59) (supplemental Tables S1 and S2 in [*Nicot et al.*, 2017]) . Data for Parker-Hood cluster, Sommervell Cluster, and samples collected outside the clusters are illustrated on a $\delta^{13}C$ vs DIC^{-1} plot (Fig.3). Anaerobic methane oxidation of stray natural gas results in a negative correlation whereby samples with higher concentrations of DIC have lower $\delta^{13}C$ values resulting from oxidation of methane with low carbon isotope values ($\delta^{13}C_{methane}$ < -25 ‰ in all samples). The measured data do not follow

this trend. Instead, samples with the highest concentration of DIC have the highest δ^{13}C value of approximately -3.6‰, which is more typical of dissolution from marine carbonates. *Grossman et al.* [1989] observed similar relationships between δ^{13}C vs DIC^{-1} from the Sparta aquifer in east Texas, but those groundwater samples contained high concentrations of methane (> 20 mg/L) with δ^{13}C values that ranged from -58.4 to -53.1‰, and very low concentrations of coexisting ethane and propane. In their study, *Grossman et al.* [1989] suggest that a combination of carbonate dissolution, acetate and CO_2 reduction methanogenesis, and anaerobic oxidation left the residual bicarbonate pool enriched in carbon-13. In this study, the methane in the Parker-Hood cluster is thermogenic in origin, but the trend of δ^{13}C vs DIC^{-1} suggests that anaerobic methane oxidation does not contribute significantly to the mass balance of bicarbonate in these waters, or is coupled to CO_2 reduction methanogenesis in such a way to offset the overall effects.

Dissolved nitrate and sulfate concentrations for groundwater samples reported by *Nicot et al.* [2017] are illustrated in Fig. 4 and Fig. 5, respectively, with respect to dissolved methane concentrations. Groundwater samples collected outside the clusters have nitrate and sulfate concentrations that are higher than observed within the clusters (Figs. 4 and 5). Sulfate was detected in all the groundwater samples analyzed, but similar to nitrate, higher concentrations of sulfate were measured outside the Parker-Hood cluster than within (Fig. 5). These data suggest anaerobic oxidation of methane coupled to nitrate, and potentially sulfate reduction occurred within the Parker-Hood cluster. *Darvari et al.* [2017] concluded, based on the distribution of trace elements in groundwater samples within the Barnett shale footprint, that anaerobic reduction of methane in the nitrate and iron stage did occur with carbonate precipitation. It is uncertain, however, how much groundwater nitrate may have existed prior to nitrate reduction and therefore the contribution of nitrate reduction to dissolved nitrogen gas is unknown. Considering that the DIC data (section 4.3) does not support significant methane oxidation, it does not appear that the alkane chemistry could have been significantly affected by subsequent anaerobic methane oxidation. In the context of applying dissolved nitrogen chemistry to attribute sources of methane and estimate source mixing ratios, however, we must consider the effect that any anaerobic oxidation of methane coupled to nitrate reduction could have on the preserved dissolved nitrogen chemistry. In the following section the dissolved nitrogen chemistry of these samples is described, and effects associated with anaerobic oxidation of methane coupled to nitrate reduction is discussed.

4.5 Dissolved nitrogen chemistry

Dissolved nitrogen concentrations and δ^{15}N values are measured at 43 locations within Parker-Hood cluster (n=21), the Somervell cluster (n=1), the North Parker cluster (n=1) and outside the clusters (n=20) (Table 2). Samples cover a range of dissolved methane concentrations from non-detect to high and elevated. Dissolved nitrogen concentrations and corresponding δ^{15}N values are listed in Table 2. Nitrogen isotope values are plotted relative to dissolved nitrogen concentration in Fig. 6. Samples collected outside the Parker-Hood cluster have δ^{15}N values that average 0.52±0.16‰ and dissolved nitrogen concentrations that range from 11.6 to 27.6 mg/L. The Mean Annual Air Temperature (MAAT) for Granbury, TX, the nearest city to the field area, is 18°C. MAAT is used as an approximation for the Water Table Temperature (WTT) that the dissolved gas in the groundwater was equilibrated with the atmosphere. Using this WTT we calculate an initial dissolved nitrogen concentration for atmospheric recharged groundwater of 14.5 mg/L and a δ^{15}N values near 0‰. Sample BS179A has a dissolved nitrogen concentration of 27.6 mg/L that is outside 2σ of the dataset and may reflect addition of excess atmospheric nitrogen during recharge, or contamination with atmospheric gas during sampling. With the exception of sample BS179A, samples outside the Parker-Hood cluster have dissolved nitrogen concentrations that average 17.5 ± 3.3 mg/L, which is slightly higher than, but within 1σ of groundwater recharged at 18°C [*Weiss*, 1970].

Samples from the Parker-Hood cluster preserve dissolved nitrogen concentrations and δ^{15}N values of a wider range than observed outside the cluster and also preserve a negative correlation (r^2=0.62) whereby samples with the highest dissolved methane concentration have the lowest dissolved nitrogen concentration (Fig. 7). Four samples (BS551, BS553, BS555, and BS355a) have dissolved nitrogen concentrations that are below 11 mg/L and cannot be explained through simple groundwater recharge equilibrated with atmosphere. These four samples also have the highest dissolved methane concentrations measured in the field area (Fig. 7) and three of these samples have dissolved nitrogen $\delta^{15}N$ values that are lower than expected for atmospheric recharged groundwater (see Fig.6). Samples within the Parker-Hood cluster that have intermediate to non-detect dissolved methane concentrations also have dissolved nitrogen chemistries that are more typical of atmospheric recharged groundwater (Figs. 6 and 7).

5 Discussion of dissolved gas processes and transport of stray natural gas

Collectively, measured alkane concentrations, $\delta^{13}C_{methane}$ values, and C1/(C2+C3) ratios of alkanes in shallow groundwater are consistent with the presence of stray natural gas in at least one cluster of groundwater wells on the border of Parker and Hood counties, and likely affected at least 3 groundwater wells in the southern Somervell cluster. A similar conclusion is reached by *Wen et al.* [2016] and *Darrah et al.* [2014] based on noble gas signatures. Sample locations outside these two clusters and throughout the entire field area have either non-detect or trace concentrations of dissolved methane. Locations with intermediate concentrations of dissolved methane also have non-detect concentrations of ethane and propane and low $\delta^{13}C_{methane}$ values that are consistent with contribution of methane from low temperature microbial processes rather than migration of stray natural gas [*Wolin and Miller*, 1987; *Whiticar*, 1999; *Zhang et al.*, 1998]. In this section we couple measured dissolved alkane and nitrogen chemistry to test the hypothesis that dissolved nitrogen may add an additional source attribution technique and discern transport processes for stray natural gas. This approach of using dissolved nitrogen chemistry builds off dissolved noble gas chemistry studies by applying the same gas partitioning processes and calculations [*Ballentine et al.*, 2002]. Namely, we explore the effects of exsolution and dissolution of insoluble gases in two-phase systems and mixing between chemically distinct reservoirs. We directly compare results obtained with nitrogen chemistry to the noble gas research of *Wen et al.* [2016] that includes samples collected from the same wells in this study. In this way, the results of nitrogen chemistry can be validated against previously published noble gas methods. The observed relationship between methane concentration and dissolved nitrogen chemistry is considered with respect to three gas-water processes that will affect the $\delta^{15}N$ value and/or concentration of dissolved nitrogen in groundwater: (1) addition of excess nitrogen from external sources, (2) stripping of dissolved nitrogen from the aqueous phase into a gas phase, and (3) exchange or mixing of nitrogen between two nitrogen-bearing reservoirs. In addition to gas-water processes, we include effects associated with microbial denitrification which may have the coupled effect of 1) increasing the dissolved nitrogen concentration, 2) changing the $\delta^{13}C_{methane}$ value of residual methane, 3) changing the C1/(C2+C3) ratios of residual alkanes, and 4) changing the dissolved nitrate, sulfate, and dissolved inorganic carbon chemistry.

Excess nitrogen can be incorporated into shallow groundwater through the inclusion of atmospheric gas bubbles during groundwater recharge [*Vogel et al.*, 1981; *Heaton and*

527 *Vogel*, 1981; *Cey et al.*, 2009] and from microbial denitrification [*Knowles*, 1982]. The

528 δ^{15}N value of atmospheric gas is close to 0‰ so the addition of excess atmospheric ni-

529 trogen would effectively increase the dissolved nitrogen concentration but not change the

530 δ^{15}N value of atmosphere-recharged groundwater. The δ^{15}N value of nitrogen sourced

531 from anaerobic microbial nitrate reduction is variable and dependent on the degree of den-

532 itrification and δ^{15}N value of the nitrate. Nitrate δ^{15}N values were not measured as part

533 of this study so it is not possible to fully assess the potential impact of this process. To

534 the south of the field area, within the Cretaceous Edwards Aquifer, dissolved nitrate δ^{15}N

535 values that range from +1.9 to +10‰ are reported with an average value of +6.2‰ [*Kre-*

536 *itler and Browning*, 1983]. Dissolved nitrate concentrations (n=118) measured in this study

537 are generally low with only 28 samples having concentrations > 5mg/L and the major-

538 ity of the samples (n=95) having non-detect dissolved nitrate concentrations. The aver-

539 age dissolved nitrate concentration measured in this study is 1.5 mg/L and the maximum

540 value measured within the Parker-Hood cluster is 4.4 mg/L. Complete reduction of an

541 initial dissolved nitrate concentration of 4.4 mg/L having a δ^{15}N value of +6.2‰ would

542 increase the δ^{15}N value and concentration of dissolved nitrogen in atmosphere-equilibrated

543 groundwater to +0.4‰ and 15.5 mg/L (starting values of 14.5 mg/L and 0‰, respec-

544 tively). Based on this estimate, the potential contribution of excess nitrogen through mi-

545 crobial denitrification is small and would not likely contribute significantly to the observed

546 nitrogen chemistry in these groundwater samples. Also, the addition of excess nitrogen, ei-

547 ther with an atmospheric or reduced nitrate δ^{15}N value, does not explain the range of data

548 observed within the Parker-Hood cluster that includes lower than expected dissolved ni-

549 trogen concentrations and δ^{15}N values. This effect is important to consider, however, and

550 is included as a possible pathway in our calculation, because it could have net effect of

551 obscuring the process of nitrogen-stripping that is described below.

552 Four groundwater wells sampled in the Parker-Hood cluster have dissolved nitrogen

553 concentrations that are below 11.0 mg/L, which is more than 2σ different than the aver-

554 age dissolved nitrogen concentration measured outside the Park Hood cluster. These four

555 groundwater wells also have the highest dissolved methane concentrations among the col-

556 lected samples. Three of these samples have the lowest measured dissolved nitrogen δ^{15}N

557 values in the dataset. This correlation between high methane and low nitrogen dissolved

558 concentrations suggests that groundwater with the lowest dissolved nitrogen concentra-

559 tions were affected by the highest degree of mixing of stray natural gas. However, nitrogen

560   stripping cannot solely account for the observed low $\delta^{15}N$ values in these three samples.

561   Infiltration of a gas that has a low concentration of nitrogen may explain the resulting low

562   dissolved nitrogen concentration in the groundwater (i.e., 'stripping'). However, isotopic

563   exchange between dissolved nitrogen and an infiltrating gas phase of nitrogen that also has

564   a low $\delta^{15}N$ value is considered to explain the observed shift in dissolved nitrogen $\delta^{15}N$

565   values.

566   Stray natural gas in this field area is likely sourced from the Barnett Shale or Strawn

567   Group. A critical difference between these two reservoirs is that natural gas from the Bar-

568   nett Shale has lower nitrogen concentrations than natural gas from the Strawn Group. In

569   the Barnett Shale nitrogen concentrations average $0.9\pm0.2\%$ with $\delta^{15}N$ values between

570   -1.8 and -7 ‰. In the Strawn Group natural gas has nitrogen concentrations that range

571   from 3.9 to 4.3%. One $\delta^{15}N$ measurement from the Strawn Group production gas is -

572   6.5‰. Stripping or exsolution of dissolved nitrogen from groundwater is driven by com-

573   positional gradients and solubility constants whereby a large compositional disequilibrium

574   between nitrogen-poor natural gas (gas-phase) and nitrogen-rich atmosphere-equilibrated

575   groundwater (aqueous phase) favors exsolution of dissolved nitrogen. Isotope exchange is

576   driven by isotope concentration gradients and isotope solubility differences, but requires

577   simultaneous exchange (i.e., exsolution and dissolution) between the gas and aqueous

578   phases. In a closed system the chemical gradient at the gas-water interface would de-

579   crease through time, inhibiting further exsolution of dissolved gas. Continued stripping

580   and exchange of dissolved nitrogen, therefore, is favored in either an open gas-phase sys-

581   tem where stray natural gas continually flushes through the groundwater system, or in a

582   closed system where a large gas to water ratio is established and maintained over long

583   periods of time. To illustrate these concepts we use an equilibrium mixing model to esti-

584   mate the relative volumes of stray natural gas and groundwater necessary to develop the

585   dissolved gas chemistry measured in this study.

586   The conceptual model is a finite volume of air saturated groundwater (dissolved ni-

587   trogen = 14.5 mg/L and $\delta^{15}N$ = +0.79 ‰ ; dissolved methane = 0.01 mg/L) that is equi-

588   librated with increasing volumes of natural gas. This mixing model is a proxy for natural

589   gas stripping of dissolved nitrogen from air saturated groundwater. Two natural gas end

590   members are investigated that are representative of the Barnett Shale (0.9% N_2 and $\delta^{15}N$

591   = -4.5‰) and the Strawn Group (5% N_2 and $\delta^{15}N$ = -6.5‰). Calculated volumetric mix-

592   ing trends for these endmembers are illustrated in Fig. 6. This is an equilibrium batch

593 model that does not account for incomplete exchange or mixing or variations in reservoir

594 temperatures and pressures; variables which are necessary to develop a fully coupled gas

595 transport model, but beyond the scope of this research. As such, this model is qualitative,

596 yet provides important insight into geochemical trends of insoluble dissolved gas species

597 and their stable isotope ratios as well as providing for comparison of the sensitivity to

598 change for different geochemical indicators. Concentration of dissolved nitrogen in the

599 mixing model is calculated using mass balance and Henry's Law constants at a constant

600 temperature and hydrostatic pressure following Eq.1:

$$mols_{N2} = C_{aq}V_{aq} + C_{gas}V_{gas} \qquad (1)$$

602 Where C_{aq} and C_{gas} are concentration of nitrogen in units of mols/L, and V_{aq} and V_{gas}

603 are their respective volumes in units of liters. Substituting the Henry's Law relationship:

$$K_H = C_{aq}/C_{gas} \qquad (2)$$

605 into Eq. 1 for C_{gas} where K_H is a dimensionless Henry's Law constant for nitrogen [*Wag-*

606 *ner and Pruss*, 1993; *Weiss*, 1970] and rearranging Eq. 1 to solve for dissolved nitrogen

607 concentration yields Eq. 3:

$$C_{aq} = \frac{mols_{N2}}{(V_{aq} + V_{gas}/K_H)} \qquad (3)$$

609 Equation 3 is analogous to Equation 2 of [*Ballentine et al.*, 1991], only solved for the con-

610 centration of a dissolved gas in an aqueous phase rather than mols of gas in the aqueous

611 phase. δ^{15}N values are solved as a mass balance between two nitrogen endmembers as-

612 suming that solubility nitrogen isotope effects are insignificant (a small fractionation factor

613 Δ^{15}N $_{gas-wat}$ = +0.7‰); will have a minor effect on this model [*Klots and Benson*, 1963].

614 Results of Equation 3 coupled to nitrogen isotope mixing are illustrated in Fig. 6 along

615 with the dissolved nitrogen data from the Parker-Hood and Sumervell clusters and samples

616 collected outside these clusters. Two gas:water mixing model trends are illustrated (solid

617 lines): one for the Barnett Shale end member (0.9% N_2 and δ^{15}N = -4.5‰) and one for

618 the Strawn Group end member (5% N_2 and δ^{15}N = -6.5‰).

619 Gas:water mixing model results demonstrate that natural gas with low nitrogen con-

620 tent, such as derived from the Barnett Shale, has a limited capacity to change the δ^{15}N

621 value of dissolved nitrogen in groundwater. In contrast, natural gas with higher nitrogen

622 content, such as from the Strawn Group, does have the capacity to change both the con-

623 centration and δ^{15}N value of dissolved nitrogen in groundwater. Samples BS555, BS553,

and BS551 from the Parker-Hood cluster have the lowest $\delta^{15}N$ values in the dataset and are interpreted as being affected by isotopic exchange with stray gas.These three samples, however, do not fall on the mixing line calculated with the Strawn Group end member. Measured nitrogen concentrations and $\delta^{15}N$ values fall to the right of the Strawn Group mixing line, suggesting that more than simple natural gas and groundwater mixing has occurred. Whereas gas:water mixing ratios that average 1:10 are required to obtain the $\delta^{15}N$ values measured for BS551 and BS553 if the natural gas was sourced from the Strawn Group, the same degree of mixing results in considerably lower calculated dissolved nitrogen concentrations than are measured. Groundwater well BS555 has the lowest measured $\delta^{15}N$ value and would require a mixing ratio approaching 1:5 assuming natural gas that is representative of the Strawn Group. As with samples BS551 and BS553, measured dissolved nitrogen concentration for BS555 is higher than calculated with the mixing model. Calculated gas-water ratios, however, are consistent with gas:water ratios reported using noble gas mixing ratios from these wells [*Wen et al.*, 2016]. Specifically, mixing ratios calculated with $^{84}Kr/^{36}Ar$ and $^{132}Xe/^{36}Ar$ vary between 1:1 and 1:4 [*Wen et al.*, 2016], consistent with the 1:5 estimate calculated here. Groundwater well BS355 which has elevated methane concentration, but atmospheric nitrogen isotope values also has visible noble gas fractionations and displays a lower gas-water ratio (1:16) calculated with noble gas ratios [*Wen et al.*, 2016] that is consistent with gas:water ratios calculated here.

Although the gas:water mixing ratios estimated using measured $\delta^{15}N$ values are in agreement with mixing ratios calculated with noble gas ratios [*Wen et al.*, 2016], the simple two component gas:water stripping model does not accurately capture the measured dissolved nitrogen concentrations, which fall to the right of the Strawn Group mixing line (Fig. 6). This suggests that either: 1) a natural gas source far richer in nitrogen than the observed from the Strawn Group exists (e.g., 15% nitrogen source illustrated in Fig. 6 for reference), 2) denitrification in methane-rich samples has added dissolved nitrogen gas that has a large $\delta^{15}N$ value, or 3) subsequent mixing of gas-stripped groundwater and atmosphere-equilibrated groundwater occurred. Lack of evidence for natural gas with such high concentrations of nitrogen in this region preclude the former hypothesis and it is not further considered. Coupled anaerobic microbial oxidation, as described in the previous section, could add a third source of nitrogen and effectively shift the measured values from the mixing line. However, data presented here suggest that effect is minimal and given the nitrate concentrations in the Trinity aquifer a maximum of 1 mg/L of

657 dissolved nitrogen could be added through denitrification. The third scenario that natural

658 gas-stripped groundwater is subsequently mixed with atmosphere equilibrated groundwater

659 is illustrated in Fig. 6 as dotted mixing lines. Linear mixing between atmosphere equili-

660 brated groundwater and three points on the Strawn Group mixing line (1:10, 1:5, and 1:2

661 mixing ratios) are illustrated. This process reasonably explains the observed data and also

662 may be expected for sampling water wells that are screened over large vertical intervals.

663 We therefore favor this coupled process as a means of explaining the measured data in

664 groundwater wells. Gas:water mixing ratios calculated using this additional mixing model

665 are 1:2 for BS555, 1:5 for BS553, and 1:10 for BS551.

666 All the other collected groundwater samples, independent of the dissolved methane

667 concentrations, have $\delta^{15}N$ values that are similar to atmospheric values and therefore do

668 not appear to have experienced the degree of gas mixing as these three samples from the

669 Parker-Hood cluster. The observed decrease in $\delta^{15}N$ does not appear to be possible with a

670 lower nitrogen-bearing gas typical of the Barnett Shale. Similar conclusions are suggested

671 for groundwater well BS199 [*Kornacki and McCaffrey*, 2014], which was not reanalyzed

672 for dissolved nitrogen in this study. Combined, these data demonstrate that only three of

673 the sampled groundwater wells preserve evidence of gas-phase transport of stray natural

674 gas into shallow groundwater. These groundwater wells are known for gas lock of pumps

675 and high levels of methane (pers. comm. with home owners). Of the other groundwater

676 wells sampled that have high dissolved methane concentrations and lower than expected

677 dissolved nitrogen concentrations, the measured $\delta^{15}N$ values of dissolved nitrogen argue

678 against large influx of stray natural gas.

679 **6 Conclusion**

680 Dissolved alkane and nitrogen concentrations, and $\delta^{15}N_{nitrogen}$ and $\delta^{13}C_{methane}$

681 values measured within the Barnett Shale natural gas play suggest that stray natural gas

682 infiltration is localized with a large cluster located near the border of Parker and Hood

683 counties. Gas dryness and $\delta^{13}C_{methane}$ values clearly point to a thermogenic natural gas

684 origin for the dissolved methane in the Parker-Hood cluster. However, these data alone

685 are not sufficient to uniquely attribute this gas to the Barnett Shale, which is the target of

686 hydraulic fracturing operations, because natural gas from the Strawn Group and Barnett

687 Shale have similar alkane chemistries. Dissolved nitrogen chemistry measured in these

688 groundwater samples an additional means to differentiate natural gas sources because of

689 differences in nitrogen concentrations between the Strawn Group and Barnett Shale.

690   Results from our dissolved nitrogen model suggest that stray gas that infiltrated the

691 groundwater in the Parker-Hood cluster likely contained higher nitrogen concentrations

692 than measured for the Barnett Shale, and are more typical of nitrogen concentrations mea-

693 sured from the Strawn Group. This conclusion is consistent with those of *Darrah et al.*

694 [2014] and *Wen et al.* [2016] who, based on noble gas signatures within groundwater in

695 Parker and Hood counties, concluded that stray natural gas in these groundwater wells

696 is more likely sourced from the Strawn Group rather than the Barnett Shale. Gas to wa-

697 ter mixing ratios as large as 1:2 are calculated for the most affected groundwater well

698 (BS555) using dissolved nitrogen chemistry. The most likely scenario we envision for af-

699 fected groundwater wells is localized transport of natural gas from the Strawn Group to

700 the shallow groundwater aquifer that occurred during groundwater well drilling. Alterna-

701 tively, isolated shallow natural gas reservoirs within the Strawn Group may be in contact

702 with groundwater aquifers within the Trinity Group along the unconformable contact these

703 rock units share.

704   Comparison of mixing model results for the alkane and nitrogen chemistry sys-

705 tems demonstrates their relative sensitivity to change. For example, groundwater equili-

706 brated with atmospheric concentrations of nitrogen and methane that is mixed with natural

707 gas with at least 5% nitrogen will require considerably less natural gas to shift its alkane

708 chemistry to the thermogenic field (1:40 mixing; see Fig. 2). With an equivalent 1:40 de-

709 gree of mixing, the nitrogen system shows an appreciable decrease in dissolved nitrogen

710 concentration (from 14 to 6.25 mg/L), but an insignificant decrease in the dissolved nitro-

711 gen δ^{15}N value. Gas to water mixing ratios larger than 1:20 are required to significantly

712 decrease the δ^{15}N value in this example system. These model results illustrate the possible

713 application of dissolved nitrogen chemistry to estimate volumetric gas:water mixing ratios

714 and add another geochemical indicator for natural gas source attribution.

720 owners who graciously provided access to their groundwater wells. The data used are

721 listed in the references and tables.

References

723 Ashworth, J., J. Hopkins, and T. W. D. Board (1995), *Aquifers of Texas*, no. 345 in

724   Aquifers of Texas, Texas Water Development Board.

725 Ball, M. M., and W. Perry (1995), Bend arch–Fort Worth basin province (045), *DL Gau-

726   tier, GL Dolton, KI Takahashi, and KL Varnes, eds*.

727 Ballentine, C., R. O'Nions, E. Oxburgh, F. Horvath, and J. Deak (1991), Rare gas con-

728   straints on hydrocarbon accumulation, crustal degassing and groundwater flow in

729   the Pannonian basin, *Earth and Planetary Science Letters*, *105*(1), 229 – 246, doi:

730   http://dx.doi.org/10.1016/0012-821X(91)90133-3.

731 Ballentine, C. J., R. Burgess, and B. Marty (2002), Tracing fluid origin, transport and in-

732   teraction in the crust, *Reviews in Mineralogy and Geochemistry*, *47*(1), 539–614.

733 Barker, J. F., and P. Fritz (1981), Carbon isotope fractionation during microbial methane

734   oxidation, *Nature*, *293*, 289–291.

735 Bernard, B., J. M. Brooks, and W. M. Sackett (1977), A geochemical model for character-

736   ization of hydrocarbon gas sources in marine sediments, in *Offshore Technology Confer-

737   ence*, Offshore Technology Conference.

738 Brown, J., L. F. (1973), Cratonic basins: terrigenous clastic models: in guidebook no. 14,

739   Pennsylvanian depositional systems in northcentral, Texas *Bur. of Econ. Geol., Austin, p.

740   10-30*.

741 Cey, B. D., G. B. Hudson, J. E. Moran, and B. R. Scanlon (2009), Evaluation of noble gas

742   recharge temperatures in a shallow unconfined aquifer, *Groundwater*, *47*(5), 646–659.

743 Chaudhuri, S., and S. Ale (2013), Characterization of groundwater resources in the Trinity

744   and Woodbine aquifers in Texas, *Science of The Total Environment*, *452-453*, 333 – 348,

745   doi:http://dx.doi.org/10.1016/j.scitotenv.2013.02.081.

746 Christian, K. M., L. K. Lautz, G. D. Hoke, D. I. Siegel, Z. Lu, and J. Kessler (2016),

747   Methane occurrence is associated with sodium-rich valley waters in domestic wells

748   overlying the Marcellus shale in New York state, *Water Resources Research*, *52*(1), 206–

749   226, doi:10.1002/2015WR017805.

750 Darrah, T. H., A. Vengosh, R. B. Jackson, N. R. Warner, and R. J. Poreda (2014), Noble

751   gases identify the mechanisms of fugitive gas contamination in drinking-water wells

752 overlying the Marcellus and Barnett shales, *Proceedings of the National Academy of Sci-*
753 *ences*, *111*(39), 14,076–14,081, doi:10.1073/pnas.1322107111.

754 Darvari, R., J.-P. Nicot, B. R. Scanlon, P. Mickler, and K. Uhlman (2017), Trace ele-
755 ment behavior in methane-rich and methane-free groundwater in north and east Texas,
756 *Groundwater*, pp. n/a–n/a, doi:10.1111/gwat.12606.

757 Eltschlager, K. K., J. W. Hawkins, W. C. Ehler, F. Baldassare, and P. Dep (2001), Techni-
758 cal measures for the investigation and mitigation of fugitive methane hazards in areas of
759 coal mining, *Department of the Interior Office of Surface Mining*.

760 Ettwig, K. F., M. K. Butler, D. Le Paslier, E. Pelletier, S. Mangenot, M. M. Kuypers,
761 F. Schreiber, B. E. Dutilh, J. Zedelius, D. De Beer, et al. (2010), Nitrite-driven anaer-
762 obic methane oxidation by oxygenic bacteria, *Nature*, *464*(7288), 543–548.

763 Fuex, A. (1980), Experimental evidence against an appreciable isotopic fractionation of
764 methane during migration, *Physics and Chemistry of the Earth*, *12*, 725–732.

765 Gilfillan, S. M., B. S. Lollar, G. Holland, D. Blagburn, S. Stevens, M. Schoell, M. Cas-
766 sidy, Z. Ding, Z. Zhou, and G. Lacrampe-Couloume (2009), Solubility trapping in for-
767 mation water as dominant CO_2 sink in natural gas fields, *Nature*, *458*, 614–618.

768 Golding, S. D., C. J. Boreham, and J. S. Esterle (2013), Stable isotope geochemistry of
769 coal bed and shale gas and related production waters: a review, *International Journal of*
770 *Coal Geology*, *120*, 24–40.

771 Grossman, E. L., B. K. Coffman, S. J. Fritz, and H. Wada (1989), Bacterial production
772 of methane and its influence on ground-water chemistry in east-central Texas aquifers,
773 *Geology*, *17*(6), 495–499.

774 Heaton, T., and J. Vogel (1981), "excess air" in groundwater, *Journal of Hydrology*, *50*,
775 201–216.

776 IHS (2015), Well completion and production reports supplied by the enerdeq
777 database, *Well completion and production reports supplied by the Enerdeq database*,
778 *https://www.ihs.com/products/oil-gas-tools-enerdeq-browser.html*.

779 Jackson, R. B., A. Vengosh, T. H. Darrah, N. R. Warner, A. Down, R. J. Poreda, S. G.
780 Osborn, K. Zhao, and J. D. Karr (2013), Increased stray gas abundance in a subset of
781 drinking water wells near Marcellus shale gas extraction, *Proceedings of the National*
782 *Academy of Sciences*, *110*(28), 11,250–11,255, doi:10.1073/pnas.1221635110.

783 Jarvie, D. M., R. J. Hill, T. E. Ruble, and R. M. Pollastro (2007), Unconventional shale-
784 gas systems: The Mississippian Barnett shale of north-central texas as one model for

thermogenic shale-gas assessment, *AAPG Bulletin*, *91*(4), 475–499.

Jenden, P., I. Kaplan, R. Poreda, and H. Craig (1988), Origin of nitrogen-rich natural gases in the California great valley: Evidence from helium, carbon and nitrogen isotope ratios, *Geochimica et Cosmochimica Acta*, *52*(4), 851 – 861, doi: https://doi.org/10.1016/0016-7037(88)90356-0.

Kampbell, D. H., and S. A. Vandegrift (1998), Analysis of dissolved methane, ethane, and ethylene in ground water by a standard gas chromatographic technique, *Journal of Chromatographic Science*, *36*(5), 253–256.

Klots, C., and B. Benson (1963), Solubilities of nitrogen, oxygen, and argon in distilled water, *Journal of Marine Research*, *21*, 48–57.

Knowles, R. (1982), Denitrification., *Microbiological Reviews*, *46*(1), 43–70.

Kornacki, A. S., and M. McCaffrey (2014), Monitoring the active migration and biodegradation of natural gas in the trinity troup aquifer at the Silverado development in southern Parker county, Texas, *AAPG 2014 Annual Conference*.

Kreitler, C. W., and L. A. Browning (1983), V.T. stringfield symposium - processes in karst hydrology nitrogen-isotope analysis of groundwater nitrate in carbonate aquifers: Natural sources versus human pollution, *Journal of Hydrology*, *61*(1), 285 – 301, doi: http://dx.doi.org/10.1016/0022-1694(83)90254-8.

Krooss, B., R. Littke, B. Müller, J. Frielingsdorf, K. Schwochau, and E. Idiz (1995), Generation of nitrogen and methane from sedimentary organic matter: implications on the dynamics of natural gas accumulations, *Chemical Geology*, *126*(3), 291–318.

Loucks, R. G., and S. C. Ruppel (2007), Mississippian Barnett shale: Lithofacies and depositional setting of a deep-water shale-gas succession in the Fort Worth basin, Texas, *AAPG bulletin*, *91*(4), 579–601.

Lu, J., T. E. Larson, and R. C. Smyth (2015), Carbon isotope effects of methane transport through Anahuac shale - a core gas study, *Journal of Geochemical Exploration*, *148*, 138–149.

Márquez, G., M. Escobar, E. Lorenzo, J. Gallego, and R. Tocco (2013), Using gas geochemistry to delineate structural compartments and assess petroleum reservoir-filling directions: A Venezuelan case study, *Journal of South American Earth Sciences*, *43*, 1–7.

Mingram, B., P. Hoth, and D. E. Harlov (2003), Nitrogen potential of Namurian shales in the north German basin, *Journal of Geochemical Exploration*, *78*, 405–408.

Molofsky, L. J., J. A. Connor, A. S. Wylie, T. Wagner, and S. K. Farhat (2013), Evaluation of methane sources in groundwater in northeastern Pennsylvania, *Groundwater*, *51*(3), 333–349.

Molofsky, L. J., S. D. Richardson, A. W. Gorody, F. Baldassare, J. A. Black, T. E. McHugh, and J. A. Connor (2016), Effect of different sampling methodologies on measured methane concentrations in groundwater samples, *Groundwater*, *54*(5), 669–680, doi:10.1111/gwat.12415.

Montgomery, S. L., D. M. Jarvie, K. A. Bowker, and R. M. Pollastro (2005), Mississippian Barnett shale, Fort Worth basin, north-central Texas: Gas-shale play with multi–trillion cubic foot potential, *AAPG bulletin*, *89*(2), 155–175.

Moritz, A., J.-F. Helie, D. L. Pinti, M. Larocque, D. Barnetche, S. Retailleau, R. Lefebvre, and Y. Gelinas (2015), Methane baseline concentrations and sources in shallow aquifers from the shale gas-prone region of the St. Lawrence lowlands (Quebec, Canada), *Environmental Science & Technology*, *49*(7), 4765–4771.

Nicot, J.P. (2013), Flow and salinity patterns in the low-transmissivity upper Paleozoic aquifers of north-central Texas, *Gulf Coast Association of Geological Societies Journal*, *2*, 53–67.

Nicot, J.P., B. R. Scanlon, R. C. Reedy, and R. A. Costley (2014), Source and fate of hydraulic fracturing water in the Barnett shale: a historical perspective, *Environmental Science & Technology*, *48*(4), 2464–2471.

Nicot, J.P., P. Mickler, T. Larson, M. Clara Castro, R. Darvari, K. Uhlman, and R. Costley (2017), Methane occurrences in aquifers overlying the Barnett shale play with a focus on Parker county, Texas, *Groundwater*, *55*, (4), 469–481.

Nordstrom, P. L. (1982), Occurrence, availability, and chemical quality of ground water in the cretaceous aquifers of north central Texas, *Report 269*, *1*.

Osborn, S. G., A. Vengosh, N. R. Warner, and R. B. Jackson (2011), Methane contamination of drinking water accompanying gas-well drilling and hydraulic fracturing, *Proceedings of the National Academy of Sciences*, *108*(20), 8172–8176, doi: 10.1073/pnas.1100682108.

Pollastro, R. M., D. M. Jarvie, R. J. Hill, and C. W. Adams (2007), Geologic framework of the Mississippian Barnett shale, Barnett-Paleozoic total petroleum system, bend arch, Fort Worth basin, Texas, *AAPG Bulletin*, *91*(4), 405–436.

Prinzhofer, A., M. R. Mello, and T. Takaki (2000), Geochemical characterization of natural gas: a physical multivariable approach and its applications in maturity and migration estimates, *AAPG Bulletin*, *84*(8), 1152–1172.

Rodriguez, N. D., and R. P. Philp (2010), Geochemical characterization of gases from the Mississippian Barnett shale, Fort Worth basin, Texas, *AAPG Bulletin*, *94*(11), 1641–1656.

Rostron, B., and S. Arkadakskiy (2014), Fingerprinting "stray" formation fluids associated and production with hydrocarbon exploration and production, *Elements*, *10*(4), 285–290, doi:10.2113/gselements.10.4.285.

Schoell, M. (1980), The hydrogen and carbon isotopic composition of methane from natural gases of various origins, *Geochimica et Cosmochimica Acta*, *44*(5), 649–661.

Siegel, D. I., N. A. Azzolina, B. J. Smith, A. E. Perry, and R. L. Bothun (2015), Methane concentrations in water wells unrelated to proximity to existing oil and gas wells in northeastern Pennsylvania, *Environmental Science & Technology*, *49*(7), 4106–4112.

Solomon, D., A. Hunt, and R. Poreda (1996), Source of radiogenic helium 4 in shallow aquifers: Implications for dating young groundwater, *Water Resources Research*, *32*(6), 1805–1813.

Stumm, W., and J. J. Morgan (2012), Aquatic chemistry: chemical equilibria and rates in natural waters. 3rd Edition, John Wiley and Sons Ltd., New York.

Thompson, H. (2012), Fracking boom spurs environmental audit, *Nature*, *485*, 556–557.

Torres, M. E., A. C. Mix, and W. D. Rugh (2005), Precise δ^{13}C analysis of dissolved inorganic carbon in natural waters using automated headspace sampling and continuous-flow mass spectrometry, *Limnol. Oceanogr.: Methods*, *3*, 349–360.

Valentine, D. L., and W. S. Reeburgh (2000), New perspectives on anaerobic methane oxidation, *Environmental Microbiology*, *2*(5), 477–484, doi:10.1046/j.1462-2920.2000.00135.x.

Vogel, J., A. Talma, and T. Heaton (1981), Gaseous nitrogen as evidence for denitrification in groundwater, *Journal of Hydrology*, *50*, 191–200.

Wagner, W., and A. Pruss (1993), International equations for the saturation properties of ordinary water substance. revised according to the international temperature scale of 1990. addendum to *Journal of Physical and Chemical Reference Data* 16, 893 (1987), *Journal of Physical and Chemical Reference Data*, *22*(3), 783–787.

Waldron, S., E. Marian Scott, L. E. Vihermaa, and J. Newton (2014), Quantifying precision and accuracy of measurements of dissolved inorganic carbon stable isotopic composition using continuous-flow isotope-ratio mass spectrometry, *Rapid Communications in Mass Spectrometry*, *28*(10), 1117–1126, doi:10.1002/rcm.6873, rCM-13-0542.R1.

Weiss, R. (1970), The solubility of nitrogen, oxygen and argon in water and seawater, pp. 721–735, Elsevier.

Wen, T., M. C. Castro, B. R. Ellis, C. M. Hall, and K. C. Lohmann (2015), Assessing compositional variability and migration of natural gas in the Antrim shale in the Michigan basin using noble gas geochemistry, *Chemical Geology*, *417*, 356–370.

Wen, T., M. C. Castro, J.-P. Nicot, C. M. Hall, T. Larson, P. J. Mickler, and R. Darvari (2016), Methane sources and migration mechanisms in shallow groundwaters in Parker and Hood counties, Texas–a heavy noble gas analysis, *Environmental Science & Technology*.

Wen, T., M. C. Castro, J.-P. Nicot, C. M. Hall, D. L. Pinti, P. Mickler, R. Darvari, and T. Larson (2017), Characterizing the noble gas isotopic composition of the Barnett shale and Strawn group and constraining the source of stray gas in the Trinity aquifer, north-central Texas, *Environmental Science & Technology*, *51*(11), 6533–6541, doi: 10.1021/acs.est.6b06447, pMID: 28486811.

Wen, T., X. Nui, M. Gonzales, G. Zheng, Z. Li, and S.L. Brantley (2018), Big groundwater data sets reveal possible rare contamination amid otherwise improved water quality for some analytes in a region of Marcellus Shale development, *Environmental Science & Technology*, doi:10.1021/acs.est.8b01123,

Whiticar, M. J. (1999), Carbon and hydrogen isotope systematics of bacterial formation and oxidation of methane, *Chemical Geology*, *161*(1), 291–314.

Wolin, M. J., and T. L. Miller (1987), Bioconversion of organic carbon to CH_4 and CO_2, *Geomicrobiology Journal*, *5*(3-4), 239–259, doi:10.1080/01490458709385972.

Zhang, C., E. L. Grossman, and J. W. Ammerman (1998), Factors influencing methane distribution in Texas ground water, *Groundwater*, *36*(1), 58–66, doi:10.1111/j.1745-6584.1998.tb01065.x.

7 Table captions

Table 1. Alkane and nitrogen gas chemistry measured from natural gas production wells sourced in the Barnett Shale and Strawn Group. Concentration is reported in percent

914 and isotope values are reported in standard permil notation. n.a. (not analyzed). n.r. (not

915 reported).

916 Table 2. Dissolved alkane and nitrogen chemistry measured from shallow groundwa-

917 ter wells in the field area. n.a. (not applicable due to below detection concentrations). b.d.

918 (below detection).

8 Figure captions

920 Figure 1. Field map showing groundwater well locations (circles) and Barnett Shale

921 natural gas production wells (small red dots). Purple triangles are producing wells that

922 were sampled in this study. Colors of the circles correspond to concentration of dissolved

923 methane and are grouped using the classification described in the text for trace, low, inter-

924 mediate, high and elevated concentrations. Parker and Hood county lines are shown, and

925 urban areas associated with the Dallas Fort Worth metroplex are highlighted in yellow.

926 Figure 2. Bernard plot [*Bernard et al.*, 1977] showing carbon isotope values and gas

927 dryness for sampled wells. Circle size correlates to concentration of dissolved methane.

928 Samples are grouped into the three clusters described in the text. Sources of produced gas

929 from Barnett Shale and Strawn Group are also shown. Two-component mixing lines be-

930 tween Barnett Shale produced natural gas and two different microbial end-member sources

931 are illustrated along with calculated volumetric gas:water mixing ratios.

932 Figure 3. Plot of carbon isotope values of DIC compared to DIC concentration^{-1} for

933 samples from the Park Hood and Somervell clusters, and outside the clusters.

934 Figure 4. Plot of nitrate concentrations compared to dissolved methane concentra-

935 tions (mg/L) for samples from the Park Hood and Somervell clusters, and outside the

936 clusters.

937 Figure 5. Plot of sulfate concentrations compared to dissolved methane concentra-

938 tions (mg/L) for samples from the Park Hood and Somervell clusters, and outside the

939 clusters.

940 Figure 6. Comparison of dissolved nitrogen $\delta^{15}N$ values and corresponding concen-

941 trations for samples collected within and near the three groundwater well clusters. Trends

942 expected for: 1) excess nitrogen, 2) stripped nitrogen, and 3) nitrogen isotope exchange

943 between thermogenic and atmospheric nitrogen are illustrated. Solid lines labeled 0.9 and

944 5% represent mixing model trends for stray gas from Barnett Shale and Strawn Group, re-

945 spectively. Bold dashed line shows mixing effects for a hypothetical natural gas with 15%

946 nitrogen. Thin dasshed lines show mixing between atmospheric and stripped groundwa-

947 ter reservoirs. Volumetric gas:water mixing ratios (calculated at standard temperature and

948 pressure) are illustrated.

949 Figure 7. Comparison of dissolved methane and nitrogen concentrations in samples

950 across the field area. Linear regression through data from the Parker-Hood cluster illus-

951 trate the negative correlation between dissolved methane and nitrogen in this area.

Figure 1.
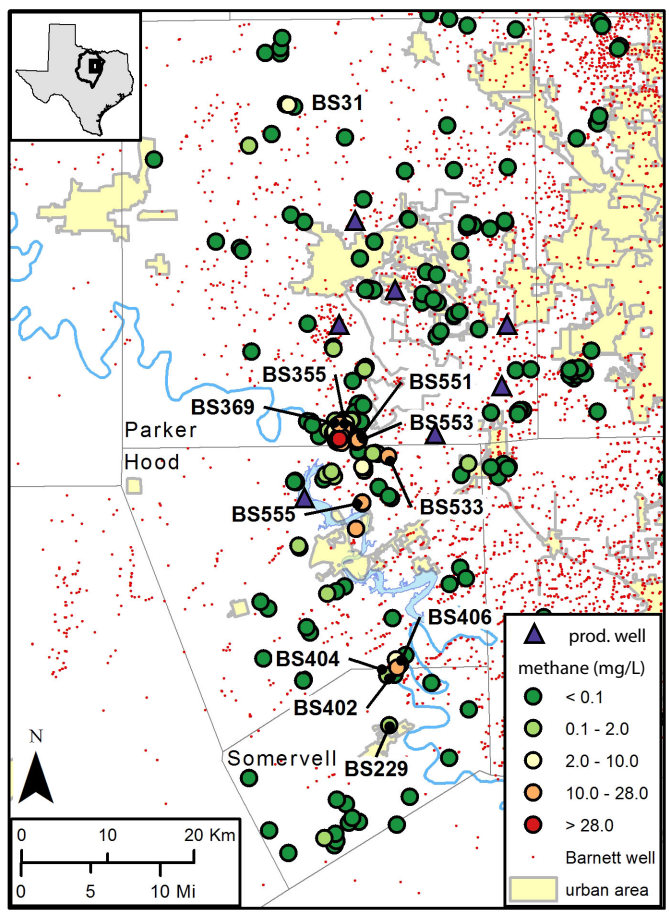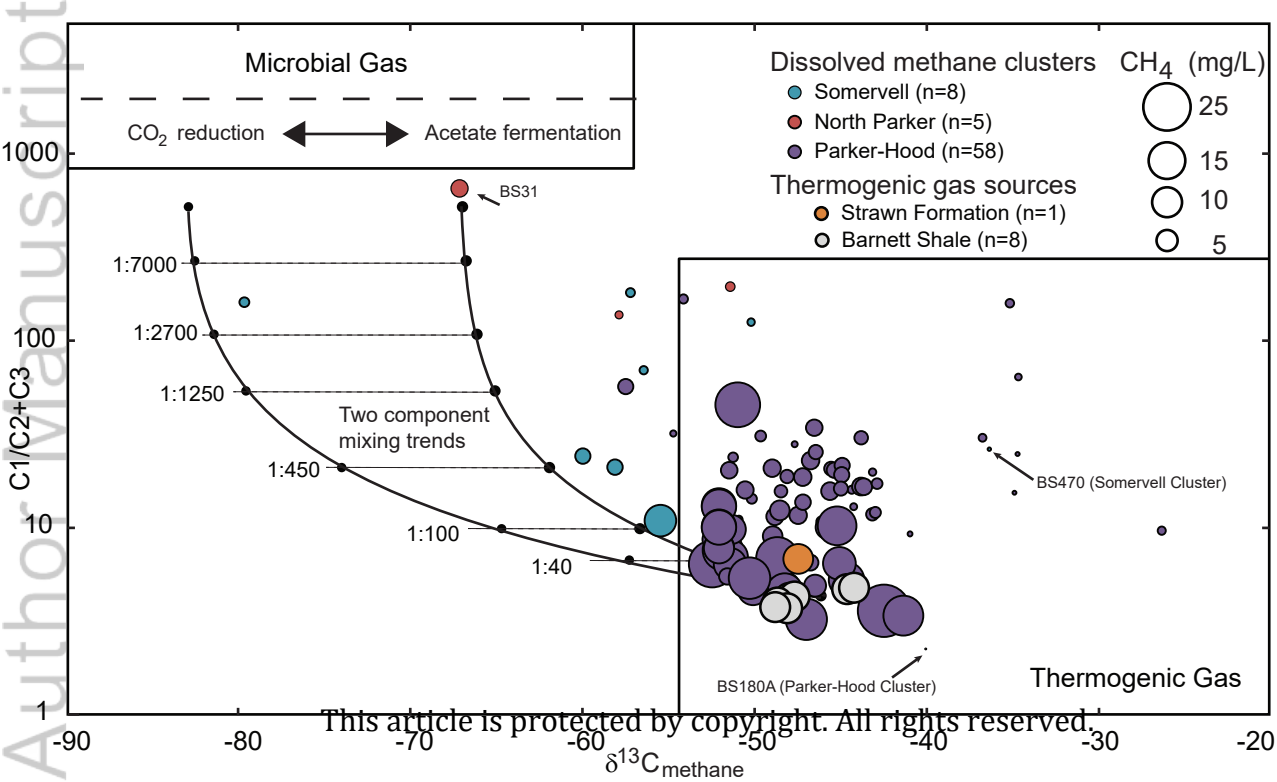
Figure 2.

Microbial Gas

CO_2 reduction ⟷ Acetate fermentation

Dissolved methane clusters
- Somervell (n=8)
- North Parker (n=5)
- Parker-Hood (n=58)

Thermogenic gas sources
- Strawn Formation (n=1)
- Barnett Shale (n=8)

CH_4 (mg/L)
- 25
- 15
- 10
- 5

BS31

1:7000
1:2700
1:1250
1:450
1:100
1:40

Two component
mixing trends

BS470 (Somervell Cluster)

BS180A (Parker-Hood Cluster)

Thermogenic Gas

C1/C2+C3

$\delta^{13}C_{methane}$

-90 -80 -70 -60 -50 -40 -30 -20

1000
100
10
1

Figure 3.

Fig.3
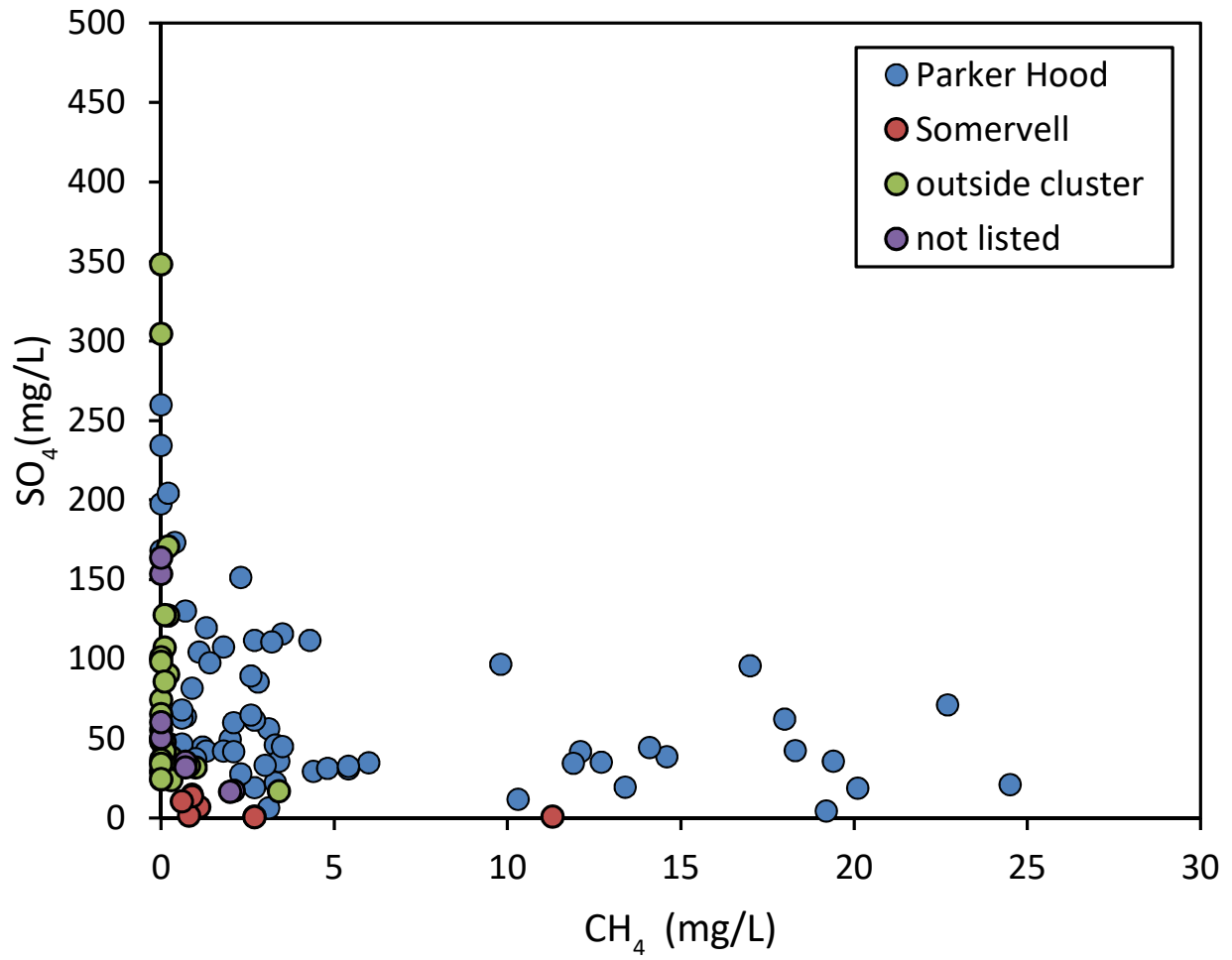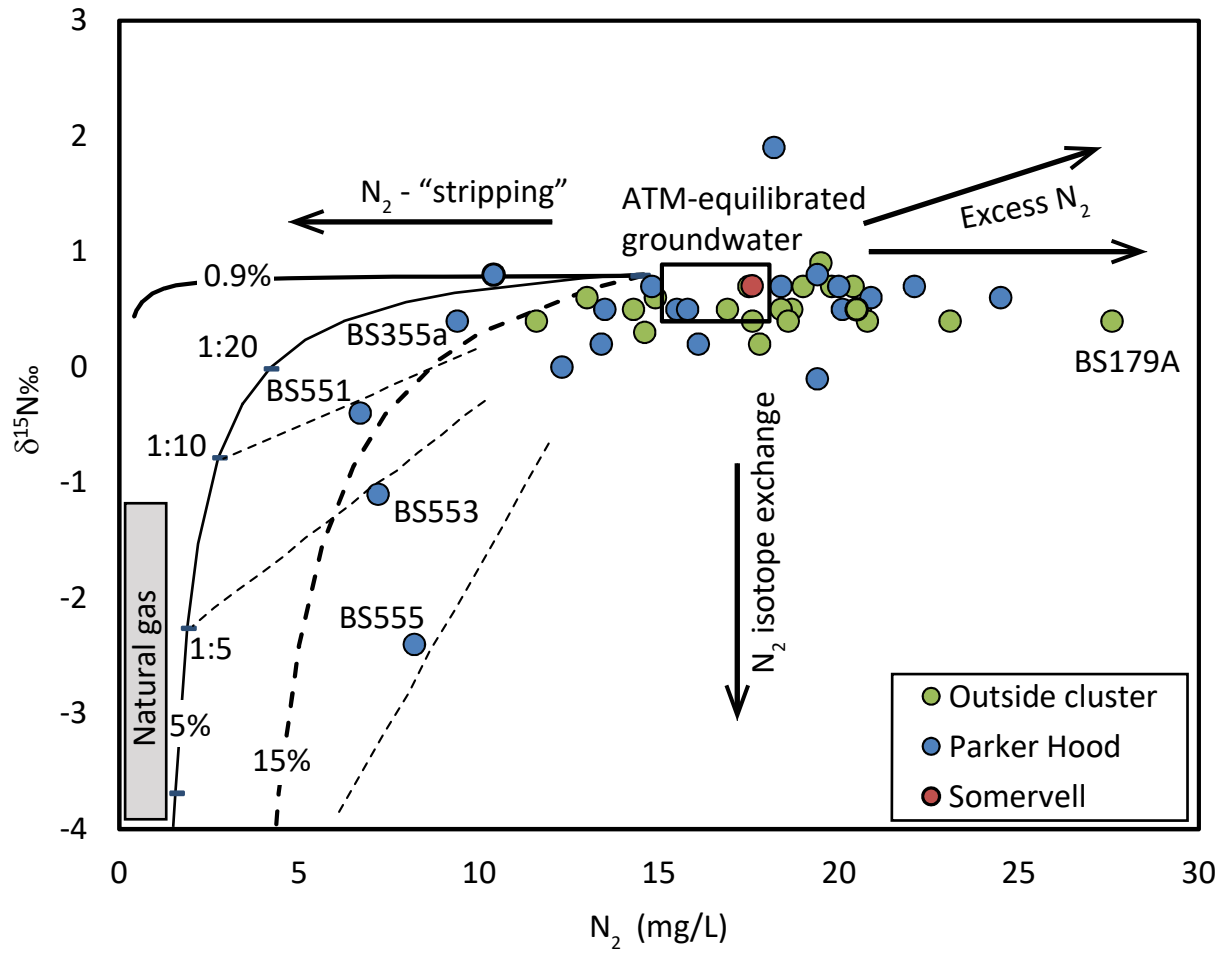
Figure 4.

Figure 5.

Figure 6.

Figure 7.
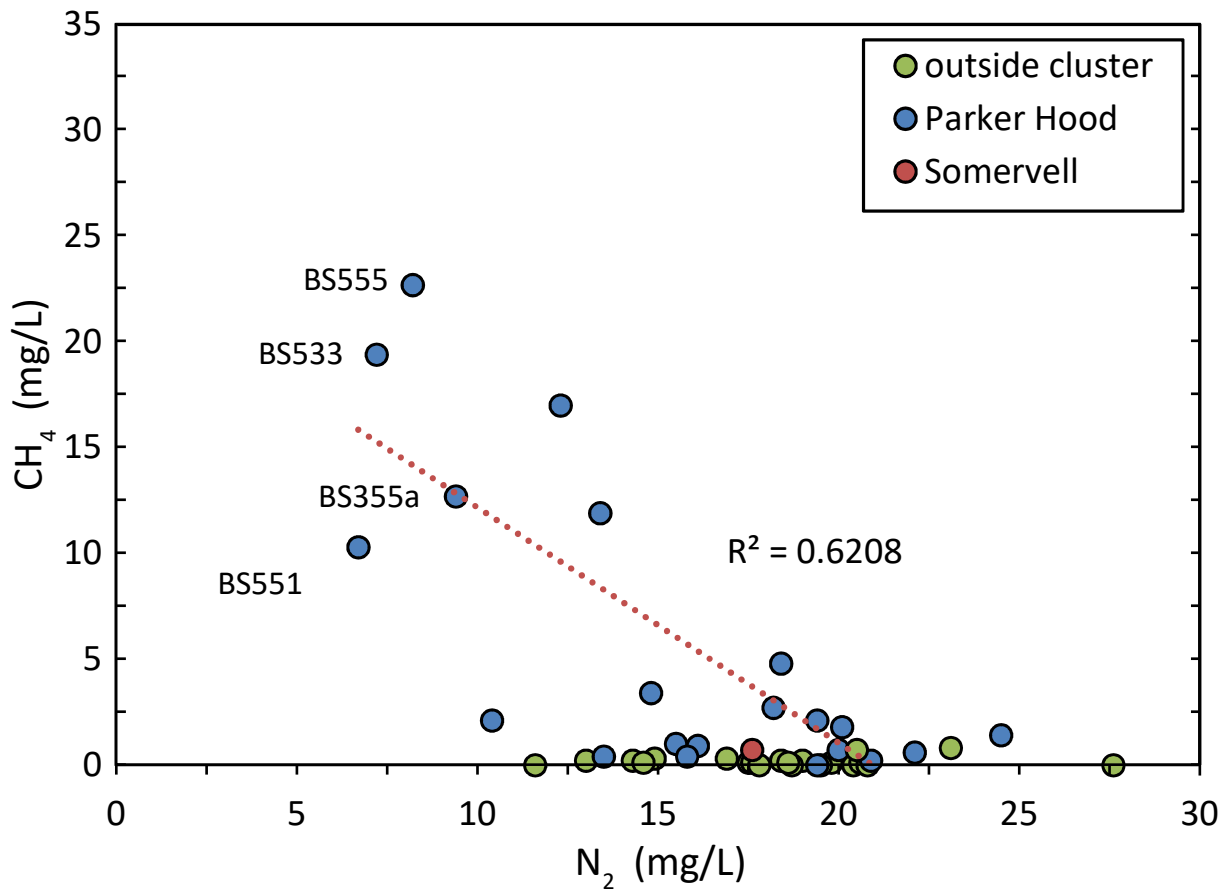
Table 1.   Alkane and nitrogen gas chemistry measured from natural gas production wells sourced in the
Concentration is reported in percent and isotope values are reported in standard permil notati

Sample	Source	County	latitude	longitude	Methane	Ethane	Propane	δ¹³C methane
BG-5	Barnett Shale	Hood	32.51	-97.84	75.1	14.4	5.4	-48
BG-6	Barnett Shale	Parker	32.66	-97.81	75.3	14.4	5.3	-48.7
BG-4	Barnett Shale	Parker	32.67	-97.8	76.5	13.8	5	-48.6
BG-9	Barnett Shale	Parker			77.2	13.5	4.6	-47.2
BG-1	Barnett Shale	Parker	32.7	-97.79	77.5	13.3	4.8	-47.9
BG-2	Barnett Shale	Parker	32.7	-97.79	77.6	13	4.7	-47.6
BG-7	Barnett Shale	Parker	32.72	-97.63	79.4	12.6	4	-44.5
BG-8	Barnett Shale	Parker	32.72	-97.63	79.7	12.4	3.9	-44.1
Barnett-1	Barnett Shale				78	12.2		-47.5
Barnett-2	Barnett Shale				72	15.4		-47.4
BG-3	Strawn Group	Parker	32.67	-97.8	82.1	8	3.9	-47.4
Strawn-1	Strawn Group				83	7.9	n.a.	-47.9
Strawn-2	Strawn Group				84	6.9	n.a.	-47.6
Strawn-3	Strawn Group				85	8	n.a.	-48.6
Strawn-4	Strawn Group				84	9.1	n.a.	-47.6

Barnett Shale and Strawn Group.
on. n.a. (not analyzed). n.r. (not reported).

N2 %	δ^{15}N N$_2$	Source
1.4	-4.2	this study
0.9	-6.1	this study
0.7	-7.7	this study
0.9	-4.1	this study
0.9	-5.69	this study
0.9	-5	this study
0.7	-2.4	this study
0.7	-1.8	this study
0.9	n.a.	Darrah et al. (2014)
1.2	n.a.	Darrah et al. (2014)
2.7	-6.5	this study
5.6	n.a.	Darrah et al. (2014)
4.6	n.a.	Darrah et al. (2014)
3.3	n.a.	Darrah et al. (2014)
3.5	n.a.	Darrah et al. (2014)

Table 2. Dissolved alkane and nitrogen chemistry measured from shallow groundwater wells in the field area. n.a. (not applicable due to below detection concentrations). b.d. (below detection).

Sample ID	Cluster	Lat	Long	Depth (ft)	methane mg/L	ethane mg/L	propane mg/L	gas wetness	$\delta^{13}C_{CH4}$ (‰)	N_2 mg/L	$\delta^{15}N$ (‰)
BS029	North Parker	32.87	-97.89	180	1	<0.002	<0.003	200	-51.3		
BS029B	North Parker	32.87	-97.89	180	0.7	<0.002	<0.003	140	-57.8		
BS031	North Parker	32.91	-97.84	170	3.4	<0.002	<0.003	680	-67.1		
BS031B	North Parker	32.91	-97.84	170	2	<0.002	<0.003	400	-67.2		
BS031C	North Parker	32.91	-97.84	170	2.1	<0.002	<0.003	420	-62.1	10.4	0.8
BS168	Outside	32.63	-97.75	400	0.1	<0.002	<0.003	20	b.d.	17.5	0.7
BS178A	Outside	32.58	-97.82	110	0.1	<0.002	<0.003	20	b.d.	19.8	0.7
BS179	Outside	32.58	-97.83	80	<0.001	<0.002	<0.003	n.a.	b.d.		
BS179A	Outside	32.58	-97.83	80	<0.001	<0.002	<0.003	n.a.	b.d.	27.6	0.4
BS197	Outside	33.06	-97.6	390	0.2	<0.002	<0.003	40	b.d.	19	0.7
BS207	Outside	32.57	-97.77	322	<0.001	<0.002	<0.003	n.a.	b.d.		
BS207A	Outside	32.57	-97.77	322	0.1	<0.002	<0.003	20	b.d.	20.6	0.5
BS229	Outside	32.26	-97.73		0.2	<0.002	<0.003	40	b.d.	13	0.6
BS232	Outside	32.14	-97.81	400	0.1	<0.002	<0.003	20	b.d.	17.6	0.4
BS254	Outside	32.97	-97.85	180	<0.001	<0.002	<0.003	n.a.	b.d.		
BS254A	Outside	32.97	-97.85	180	<0.001	<0.002	<0.003	n.a.	b.d.	20.4	0.7
BS255	Outside	32.96	-97.87	360	<0.001	<0.002	<0.003	n.a.	b.d.		
BS255A	Outside	32.96	-97.87	360	<0.001	<0.002	<0.003	n.a.	b.d.	19.5	0.9
BS311	Outside	32.4	-97.81	357	0.3	<0.002	<0.003	60	b.d.	16.9	0.5
BS338	Outside	32.54	-97.75	440	0.1	<0.002	<0.003	20	b.d.	14.6	0.3
BS338A	Outside	32.54	-97.75	440	<0.001	<0.002	<0.003	n.a.	b.d.	17.8	0.2
BS343	Outside	32.44	-97.33	100	0.2	<0.002	<0.003	40	b.d.	14.3	0.5
BS351	Outside	32.58	-97.77	345	<0.001	<0.002	<0.003	n.a.	b.d.		
BS351A	Outside	32.58	-97.77	345	0.1	<0.002	<0.003	20	b.d.	18.6	0.4
BS352	Outside	32.57	-97.78		0.3	<0.002	<0.003	60	b.d.	14.9	0.6
BS364A	Outside	32.59	-97.76	325	<0.001	<0.002	<0.003	n.a.	b.d.		
BS365	Outside	32.59	-97.76	375	<0.001	<0.002	<0.003	n.a.	b.d.		
BS365A	Outside	32.59	-97.76	375	<0.001	<0.002	<0.003	n.a.	b.d.	18.7	0.5
BS367A	Outside	32.6	-97.76		<0.001	<0.002	<0.003	n.a.	b.d.		
BS370	Outside	32.52	-97.8	220	0.2	<0.002	<0.003	40	b.d.	18.4	0.5
BS446	Outside	32.58	-97.77	100	<0.001	<0.002	<0.003	n.a.	b.d.		
BS446A	Outside	32.58	-97.77	100	<0.001	<0.002	<0.003	n.a.	b.d.	20.8	0.4
BS534	Outside	32.46	-97.77	275	<0.001	<0.002	<0.003	n.a.	b.d.		
BS534B	Outside	32.46	-97.77	275	<0.001	<0.002	<0.003	n.a.	b.d.		
BS534C	Outside	32.46	-97.77	275	<0.001	<0.002	<0.003	n.a.	b.d.	11.6	0.4
BS554	Outside	32.56	-97.77	320	0.8	<0.002	<0.003	160	b.d.	23.1	0.4
BS016B	Parker Hood	32.57	-97.8	150	0.7	<0.002	<0.003	140	-44.3		
BS016C	Parker Hood	32.57	-97.8	150	0.6	<0.002	<0.003	120	-48.8	22.1	0.7
BS017	Parker Hood	32.57	-97.79	175	<0.001	<0.002	<0.003	n.a.	b.d.		
BS017B	Parker Hood	32.57	-97.79	175	0.2	<0.002	<0.003	40	-34.6		
BS017C	Parker Hood	32.57	-97.79	175	<0.001	<0.002	<0.003	n.a.	b.d.		
BS112A	Parker Hood	32.57	-97.8		0.7	0.1	<0.003	7	-26.2	20	0.7

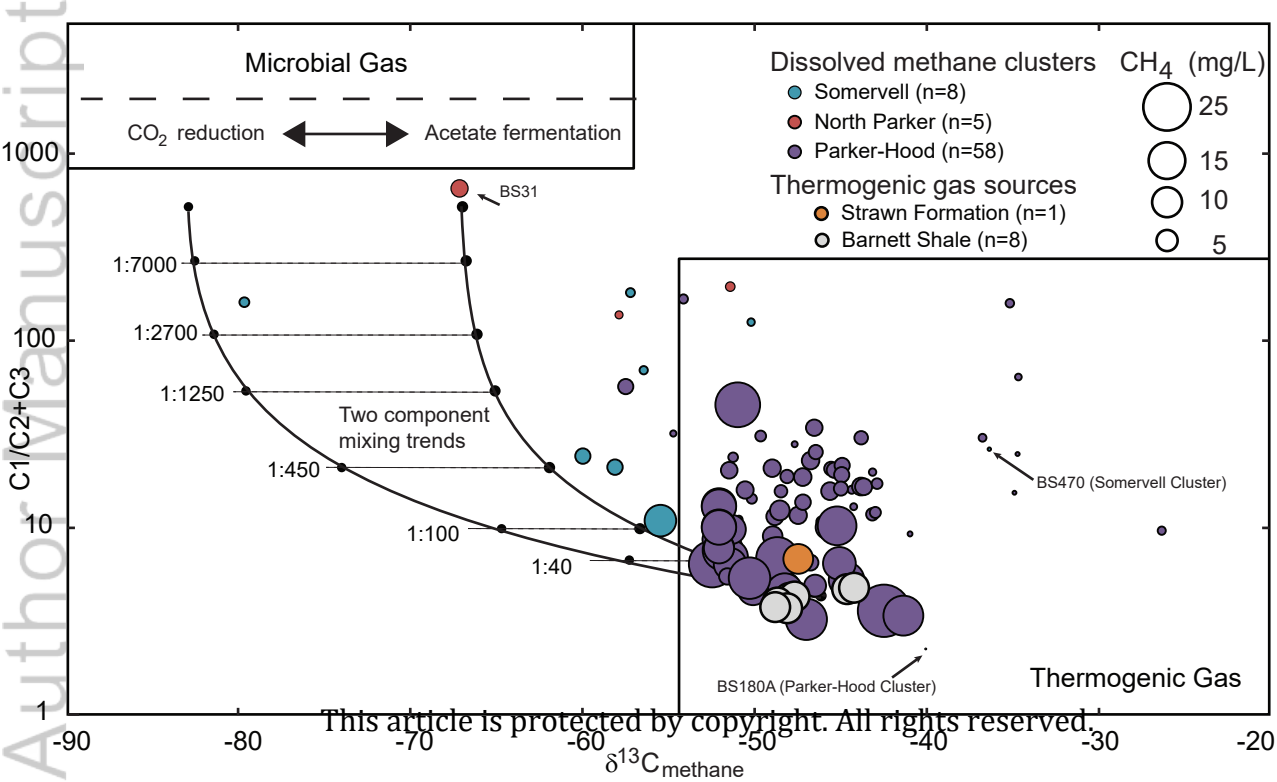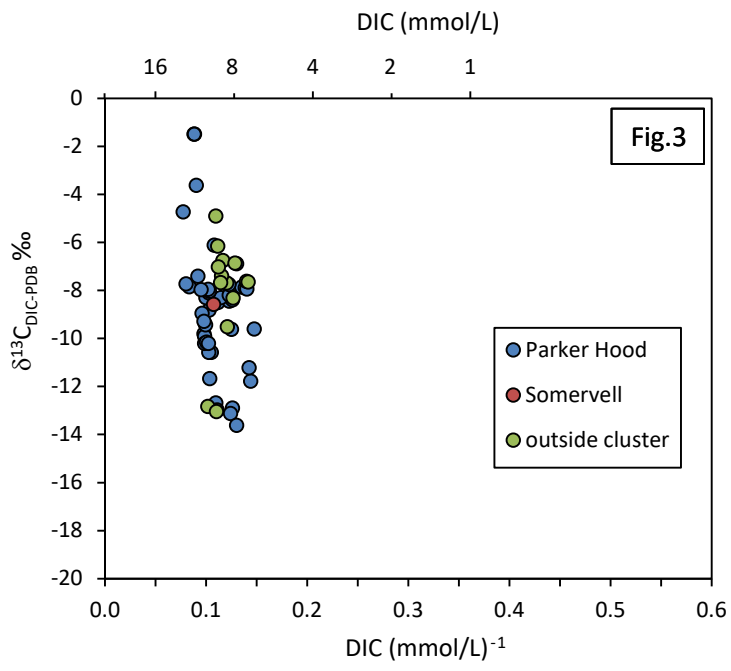| Sample ID	Cluster	Lat	Long	Depth (ft)	methane mg/L	ethane mg/L	propane mg/L	gas wetness	$\delta^{13}C_{CH4}$ (‰)	N_2 mg/L	$\delta^{15}N$ (‰)
BS175	Parker Hood	32.65	-97.79	285	0.4	<0.002	<0.003	80	-54.7	13.5	0.5
BS180	Parker Hood	32.58	-97.82	320	<0.001	<0.002	<0.003	n.a.	b.d.		
BS180A	Parker Hood	32.58	-97.82	320	<0.001	<0.002	<0.003	n.a.	-40	19.4	0.8
BS199	Parker Hood	32.56	-97.79	180	31	6.2	2.2	4	-42.4		
BS199B	Parker Hood	32.56	-97.79	180	19.2	4.3	1.6	3	-46.9		
BS200	Parker Hood	32.55	-97.78	368	24.5	3.7	<0.003	7	-52.4		
BS200B	Parker Hood	32.55	-97.78	368	18.3	2.3	<0.003	8	-51.8		
BS201	Parker Hood	32.56	-97.77	470	5.4	0.9	0.2	5	-46.4		
BS201B	Parker Hood	32.56	-97.77	470	5.4	0.9	0.2	5	-48		
BS201C	Parker Hood	32.56	-97.77	470	5.1	0.9	0.2	5	-49.7		
BS202	Parker Hood	32.56	-97.78	186	14.1	2.1	0.6	5	-44.6		
BS204	Parker Hood	32.56	-97.79	200	3.5	0.2	<0.003	17	-43.7		
BS204B	Parker Hood	32.56	-97.79	200	3.2	0.2	<0.003	16	-43.6		
BS204C	Parker Hood	32.56	-97.79	200	3.5	0.2	<0.003	17	-45.5		
BS205	Parker Hood	32.56	-97.79	200	4.3	0.5	<0.003	9	-48.9		
BS206	Parker Hood	32.58	-97.77		0.6	<0.002	<0.003	120	-50.8		
BS208	Parker Hood	32.56	-97.79	210	2.1	0.1	<0.003	20	-45.5		
BS208B	Parker Hood	32.56	-97.79	210	2.7	0.1	<0.003	26	-45.3		
BS209	Parker Hood	32.56	-97.78	285	2.6	0.1	<0.003	25	-44.8		
BS209B	Parker Hood	32.56	-97.78	285	2.7	0.1	<0.003	26	-44.9		
BS210	Parker Hood	32.56	-97.79	130	0.4	<0.002	<0.003	80	-47.6	15.8	0.5
BS211	Parker Hood	32.57	-97.78	350	3.5	0.1	<0.003	34	-48.9		
BS211B	Parker Hood	32.57	-97.78	350	3.6	0.2	<0.003	18	-47.1		
BS211C	Parker Hood	32.57	-97.78	350	3.4	0.1	<0.003	33	-46.7	14.8	0.7
BS221	Parker Hood	32.56	-97.79	120	2.8	0.4	<0.003	7	-46.7		
BS222	Parker Hood	32.56	-97.78	183	2.3	0.1	<0.003	22	-46.4		
BS244	Parker Hood	32.45	-97.84		0.9	0.1	<0.003	9	-51.1		
BS340	Parker Hood	32.54	-97.74		1.3	<0.002	<0.003	260	-49.6		
BS340A	Parker Hood	32.54	-97.74		1	<0.002	<0.003	200	-51.2	15.5	0.5
BS347	Parker Hood	32.57	-97.79	240	2.3	0.1	<0.003	22	-44.9		
BS347A	Parker Hood	32.57	-97.79	240	2.7	0.2	<0.003	13	-47.1	18.2	1.9
BS348	Parker Hood	32.57	-97.78		2	0.1	<0.003	19	-48		
BS348A	Parker Hood	32.57	-97.78		1.8	0.1	<0.003	17	-48.4	20.1	0.5
BS349	Parker Hood	32.52	-97.79	199	0.6	<0.002	<0.003	120	-44.2		
BS353	Parker Hood	32.58	-97.79	270	0.6	<0.002	<0.003	120	-43.1		
BS354	Parker Hood	32.58	-97.77	380	<0.001	<0.002	<0.003	n.a.	b.d.		
BS354A	Parker Hood	32.58	-97.77	380	0.2	<0.002	<0.003	40	-34.8	20.9	0.6
BS355	Parker Hood	32.57	-97.78	225	20.1	2.7	0.1	7	-48.6		
BS355A	Parker Hood	32.57	-97.78	225	12.7	1.8	<0.003	7	-51.3	9.4	0.4
BS356	Parker Hood	32.56	-97.79		1.8	0.1	<0.003	17	-43.1		
BS356A	Parker Hood	32.56	-97.79		1.4	0.1	<0.003	14	-42.9	24.5	0.6
BS357	Parker Hood	32.57	-97.79	240	3.1	0.1	<0.003	30	-46.4		
BS357A	Parker Hood	32.57	-97.79	240	2.1	0.1	<0.003	20	-43.7	19.4	-0.1
BS358	Parker Hood	32.57	-97.78	360	14.6	2.2	0.9	5	-48.2		

Sample ID	Cluster	Lat	Long	Depth (ft)	methane mg/L	ethane mg/L	propane mg/L	gas wetness	$\delta^{13}C_{CH4}$ (‰)	N_2 mg/L	$\delta^{15}N$ (‰)
BS358A	Parker Hood	32.57	-97.78	360	18	3.5	1.7	3	-41.3		
BS360	Parker Hood	32.58	-97.78	322	1.2	0.1	<0.003	12	-46		
BS361	Parker Hood	32.57	-97.79	210	3.3	0.3	<0.003	11	-48.7		
BS362	Parker Hood	32.56	-97.79	180	4.4	0.3	<0.003	15	-48.5		
BS363	Parker Hood	32.56	-97.79	120	1.3	0.1	<0.003	13	-42.8		
BS369	Parker Hood	32.57	-97.79	300	12.1	1.7	0.2	6	-45		
BS369A	Parker Hood	32.57	-97.79	300	11.9	1.7	0.2	6	-51.4	13.4	0.2
BS434	Parker Hood	32.57	-97.79		6	0.6	<0.003	10	-45.7		
BS434A	Parker Hood	32.57	-97.79		4.8	0.5	0.1	8	-52.4	18.4	0.7
BS435	Parker Hood	32.52	-97.8	180	0.3	<0.002	<0.003	60	-40.9		
BS436	Parker Hood	32.52	-97.76	320	1.1	0.1	<0.003	11	-50.1		
BS443	Parker Hood	32.53	-97.76	420	3.3	0.2	<0.003	16	-50.5		
BS444	Parker Hood	32.53	-97.76	220	3.1	0.1	<0.003	30	-51.4		
BS447	Parker Hood	32.58	-97.77		0.5	<0.002	<0.003	100	-34.6		
BS447A	Parker Hood	32.58	-97.77		0.7	<0.002	<0.003	140	-36.7	20.5	0.5
BS448	Parker Hood	32.58	-97.77		0.8	<0.002	<0.003	160	-35.1		
BS533	Parker Hood	32.54	-97.73	500	9.8	0.9	0.1	10	-51.3		
BS533B	Parker Hood	32.54	-97.73	500	13.4	1	<0.003	13	-52		
BS533C	Parker Hood	32.54	-97.73	500	17	1.6	0.1	10	-45.1	12.3	0
BS544	Parker Hood	32.49	-97.76	420	2.6	<0.002	<0.003	520	-57.4		
BS544A	Parker Hood	32.49	-97.76	420	0.9	<0.002	<0.003	180	-54.1	16.1	0.2
BS551	Parker Hood	32.56	-97.76	363	10.3	1.8	0.3	5	-50	6.7	-0.4
BS552	Parker Hood	32.56	-97.76	385	3	0.4	0.1	6	-51.5		
BS553	Parker Hood	32.56	-97.76		19.4	2.8	0.7	6	-50.2	7.2	-1.1
BS555	Parker Hood	32.49	-97.76	310	22.7	0.4	0.1	45	-50.9	8.2	-2.4
BS237	Somervell	32.31	-97.73	1350	0.6	<0.002	<0.003	120	-50.1	17.6	0.7
BS307	Somervell	32.32	-97.72	425	11.3	0.8	0.2	11	-55.4		
BS402	Somervell	32.32	-97.72	186	1.1	<0.002	<0.003	220	-79.6		
BS403	Somervell	32.33	-97.72	380	2.7	0.1	<0.003	26	-58.1		
BS404	Somervell	32.32	-97.72	370	0.8	0	<0.003	267	-56.4		
BS405	Somervell	32.33	-97.72	500	2.7	0.1	<0.003	26	-59.9		
BS406	Somervell	32.32	-97.72	395	0.9	<0.002	<0.003	180	-57.1		

Fig.3

Table 1. Alkane and nitrogen gas chemistry measured from natural gas production wells sourced in the Barnett Shale and Strawn Group. Concentration is reported in percent and isotope values are reported in standard permil notation. n.a. (not analyzed). n.r. (not reported).

Sample	Source	County	latitude	longitude	Methane	Ethane	Propane	$\delta^{13}C$ methane	N2 %	$\delta^{15}N\ N_2$	Source
BG-5	Barnett Shale	Hood	32.51	-97.84	75.1	14.4	5.4	-48	1.4	-4.2	this study
BG-6	Barnett Shale	Parker	32.66	-97.81	75.3	14.4	5.3	-48.7	0.9	-6.1	this study
BG-4	Barnett Shale	Parker	32.67	-97.8	76.5	13.8	5	-48.6	0.7	-7.7	this study
BG-9	Barnett Shale	Parker			77.2	13.5	4.6	-47.2	0.9	-4.1	this study
BG-1	Barnett Shale	Parker	32.7	-97.79	77.5	13.3	4.8	-47.9	0.9	-5.69	this study
BG-2	Barnett Shale	Parker	32.7	-97.79	77.6	13	4.7	-47.6	0.9	-5	this study
BG-7	Barnett Shale	Parker	32.72	-97.63	79.4	12.6	4	-44.5	0.7	-2.4	this study
BG-8	Barnett Shale	Parker	32.72	-97.63	79.7	12.4	3.9	-44.1	0.7	-1.8	this study
Barnett-1	Barnett Shale				78	12.2		-47.5	0.9	n.a.	Darrah et al. (2014)
Barnett-2	Barnett Shale				72	15.4		-47.4	1.2	n.a.	Darrah et al. (2014)
BG-3	Strawn Group	Parker	32.67	-97.8	82.1	8	3.9	-47.4	2.7	-6.5	this study
Strawn-1	Strawn Group				83	7.9	n.a.	-47.9	5.6	n.a.	Darrah et al. (2014)
Strawn-2	Strawn Group				84	6.9	n.a.	-47.6	4.6	n.a.	Darrah et al. (2014)
Strawn-3	Strawn Group				85	8	n.a.	-48.6	3.3	n.a.	Darrah et al. (2014)
Strawn-4	Strawn Group				84	9.1	n.a.	-47.6	3.5	n.a.	Darrah et al. (2014)

Table 2. Dissolved alkane and nitrogen chemistry measured from shallow groundwater wells in the field area. n.a. (not applicable due to below detection concentrations). b.d. (below detection).
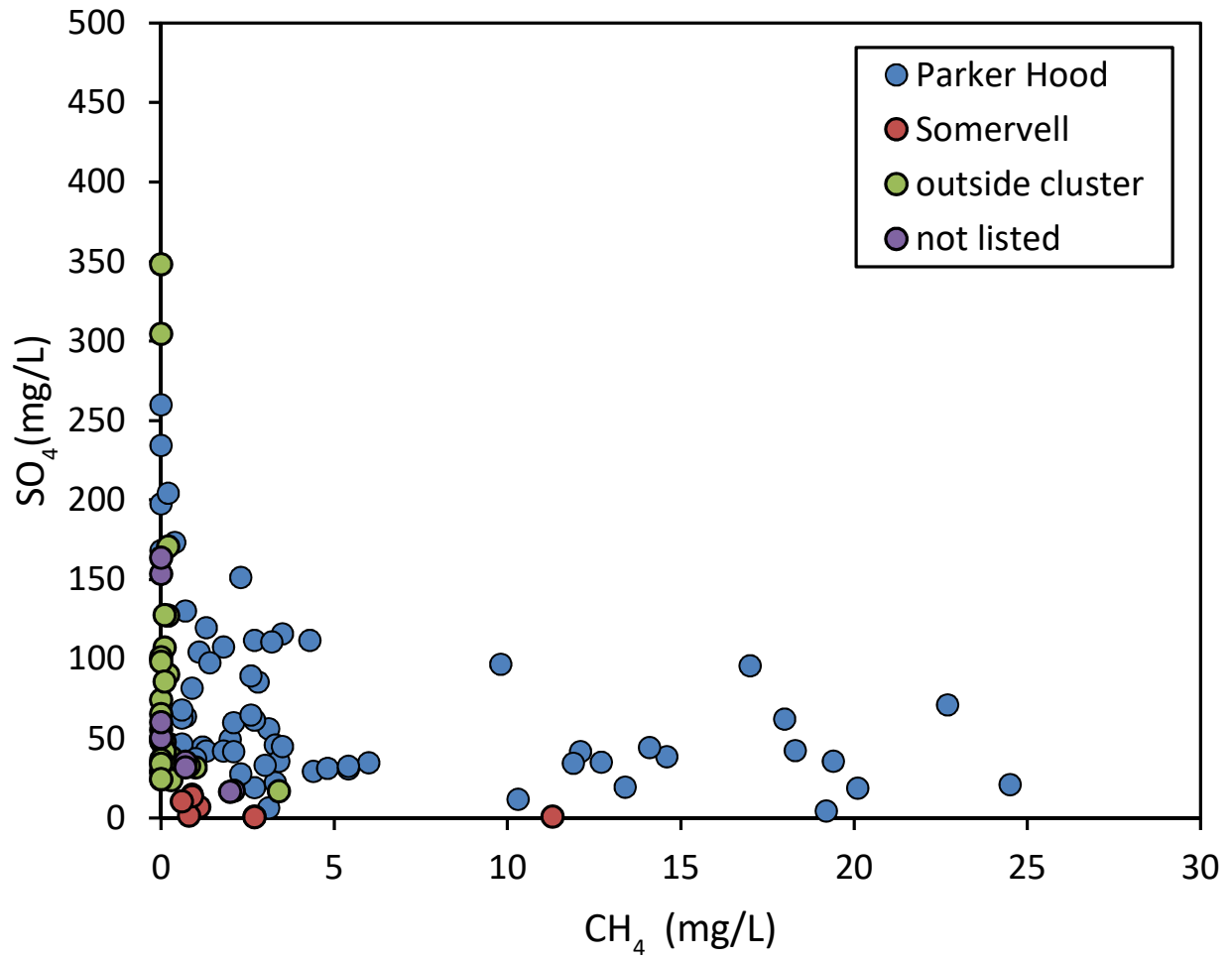
Sample ID	Cluster	Lat	Long	Depth (ft)	methane mg/L	ethane mg/L	propane mg/L	gas wetness	$\delta^{13}C_{CH4}$ (‰)	N_2 mg/L	$\delta^{15}N$ (‰)
BS029	North Parker	32.87	-97.89	180	1	<0.002	<0.003	200	-51.3		
BS029B	North Parker	32.87	-97.89	180	0.7	<0.002	<0.003	140	-57.8		
BS031	North Parker	32.91	-97.84	170	3.4	<0.002	<0.003	680	-67.1		
BS031B	North Parker	32.91	-97.84	170	2	<0.002	<0.003	400	-67.2		
BS031C	North Parker	32.91	-97.84	170	2.1	<0.002	<0.003	420	-62.1	10.4	0.8
BS168	Outside	32.63	-97.75	400	0.1	<0.002	<0.003	20	b.d.	17.5	0.7
BS178A	Outside	32.58	-97.82	110	0.1	<0.002	<0.003	20	b.d.	19.8	0.7
BS179	Outside	32.58	-97.83	80	<0.001	<0.002	<0.003	n.a.	b.d.		
BS179A	Outside	32.58	-97.83	80	<0.001	<0.002	<0.003	n.a.	b.d.	27.6	0.4
BS197	Outside	33.06	-97.6	390	0.2	<0.002	<0.003	40	b.d.	19	0.7
BS207	Outside	32.57	-97.77	322	<0.001	<0.002	<0.003	n.a.	b.d.		
BS207A	Outside	32.57	-97.77	322	0.1	<0.002	<0.003	20	b.d.	20.6	0.5
BS229	Outside	32.26	-97.73		0.2	<0.002	<0.003	40	b.d.	13	0.6
BS232	Outside	32.14	-97.81	400	0.1	<0.002	<0.003	20	b.d.	17.6	0.4
BS254	Outside	32.97	-97.85	180	<0.001	<0.002	<0.003	n.a.	b.d.		
BS254A	Outside	32.97	-97.85	180	<0.001	<0.002	<0.003	n.a.	b.d.	20.4	0.7
BS255	Outside	32.96	-97.87	360	<0.001	<0.002	<0.003	n.a.	b.d.		
BS255A	Outside	32.96	-97.87	360	<0.001	<0.002	<0.003	n.a.	b.d.	19.5	0.9
BS311	Outside	32.4	-97.81	357	0.3	<0.002	<0.003	60	b.d.	16.9	0.5
BS338	Outside	32.54	-97.75	440	0.1	<0.002	<0.003	20	b.d.	14.6	0.3
BS338A	Outside	32.54	-97.75	440	<0.001	<0.002	<0.003	n.a.	b.d.	17.8	0.2
BS343	Outside	32.44	-97.33	100	0.2	<0.002	<0.003	40	b.d.	14.3	0.5
BS351	Outside	32.58	-97.77	345	<0.001	<0.002	<0.003	n.a.	b.d.		
BS351A	Outside	32.58	-97.77	345	0.1	<0.002	<0.003	20	b.d.	18.6	0.4
BS352	Outside	32.57	-97.78		0.3	<0.002	<0.003	60	b.d.	14.9	0.6
BS364A	Outside	32.59	-97.76	325	<0.001	<0.002	<0.003	n.a.	b.d.		
BS365	Outside	32.59	-97.76	375	<0.001	<0.002	<0.003	n.a.	b.d.		
BS365A	Outside	32.59	-97.76	375	<0.001	<0.002	<0.003	n.a.	b.d.	18.7	0.5
BS367A	Outside	32.6	-97.76		<0.001	<0.002	<0.003	n.a.	b.d.		
BS370	Outside	32.52	-97.8	220	0.2	<0.002	<0.003	40	b.d.	18.4	0.5
BS446	Outside	32.58	-97.77	100	<0.001	<0.002	<0.003	n.a.	b.d.		
BS446A	Outside	32.58	-97.77	100	<0.001	<0.002	<0.003	n.a.	b.d.	20.8	0.4
BS534	Outside	32.46	-97.77	275	<0.001	<0.002	<0.003	n.a.	b.d.		
BS534B	Outside	32.46	-97.77	275	<0.001	<0.002	<0.003	n.a.	b.d.		
BS534C	Outside	32.46	-97.77	275	<0.001	<0.002	<0.003	n.a.	b.d.	11.6	0.4
BS554	Outside	32.56	-97.77	320	0.8	<0.002	<0.003	160	b.d.	23.1	0.4
BS016B	Parker Hood	32.57	-97.8	150	0.7	<0.002	<0.003	140	-44.3		
BS016C	Parker Hood	32.57	-97.8	150	0.6	<0.002	<0.003	120	-48.8	22.1	0.7
BS017	Parker Hood	32.57	-97.79	175	<0.001	<0.002	<0.003	n.a.	b.d.		
BS017B	Parker Hood	32.57	-97.79	175	0.2	<0.002	<0.003	40	-34.6		
BS017C	Parker Hood	32.57	-97.79	175	<0.001	<0.002	<0.003	n.a.	b.d.		
BS112A	Parker Hood	32.57	-97.8		0.7	0.1	<0.003	7	-26.2	20	0.7
BS175	Parker Hood	32.65	-97.79	285	0.4	<0.002	<0.003	80	-54.7	13.5	0.5
BS180	Parker Hood	32.58	-97.82	320	<0.001	<0.002	<0.003	n.a.	b.d.		
BS180A	Parker Hood	32.58	-97.82	320	<0.001	<0.002	<0.003	n.a.	-40	19.4	0.8
BS199	Parker Hood	32.56	-97.79	180	31	6.2	2.2	4	-42.4		
BS199B	Parker Hood	32.56	-97.79	180	19.2	4.3	1.6	3	-46.9		
BS200	Parker Hood	32.55	-97.78	368	24.5	3.7	<0.003	7	-52.4		
BS200B	Parker Hood	32.55	-97.78	368	18.3	2.3	<0.003	8	-51.8		
BS201	Parker Hood	32.56	-97.77	470	5.4	0.9	0.2	5	-46.4		
BS201B	Parker Hood	32.56	-97.77	470	5.4	0.9	0.2	5	-48		
BS201C	Parker Hood	32.56	-97.77	470	5.1	0.9	0.2	5	-49.7		
BS202	Parker Hood	32.56	-97.78	186	14.1	2.1	0.6	5	-44.6		
BS204	Parker Hood	32.56	-97.79	200	3.5	0.2	<0.003	17	-43.7		
BS204B	Parker Hood	32.56	-97.79	200	3.2	0.2	<0.003	16	-43.6		
BS204C	Parker Hood	32.56	-97.79	200	3.5	0.2	<0.003	17	-45.5		
BS205	Parker Hood	32.56	-97.79	200	4.3	0.5	<0.003	9	-48.9		
BS206	Parker Hood	32.58	-97.77		0.6	<0.002	<0.003	120	-50.8		
BS208	Parker Hood	32.56	-97.79	210	2.1	0.1	<0.003	20	-45.5		
BS208B	Parker Hood	32.56	-97.79	210	2.7	0.1	<0.003	26	-45.3		
BS209	Parker Hood	32.56	-97.78	285	2.6	0.1	<0.003	25	-44.8		
BS209B	Parker Hood	32.56	-97.78	285	2.7	0.1	<0.003	26	-44.9		
BS210	Parker Hood	32.56	-97.79	130	0.4	<0.002	<0.003	80	-47.6	15.8	0.5
BS211	Parker Hood	32.57	-97.78	350	3.5	0.1	<0.003	34	-48.9		
BS211B	Parker Hood	32.57	-97.78	350	3.6	0.2	<0.003	18	-47.1		
BS211C	Parker Hood	32.57	-97.78	350	3.4	0.1	<0.003	33	-46.7	14.8	0.7
BS221	Parker Hood	32.56	-97.79	120	2.8	0.4	<0.003	7	-46.7		
BS222	Parker Hood	32.56	-97.78	183	2.3	0.1	<0.003	22	-46.4		
BS244	Parker Hood	32.45	-97.84		0.9	0.1	<0.003	9	-51.1		
BS340	Parker Hood	32.54	-97.74		1.3	<0.002	<0.003	260	-49.6		
BS340A	Parker Hood	32.54	-97.74		1	<0.002	<0.003	200	-51.2	15.5	0.5
BS347	Parker Hood	32.57	-97.79	240	2.3	0.1	<0.003	22	-44.9		
BS347A	Parker Hood	32.57	-97.79	240	2.7	0.2	<0.003	13	-47.1	18.2	1.9
BS348	Parker Hood	32.57	-97.78		2	0.1	<0.003	19	-48		
BS348A	Parker Hood	32.57	-97.78		1.8	0.1	<0.003	17	-48.4	20.1	0.5
BS349	Parker Hood	32.52	-97.79	199	0.6	<0.002	<0.003	120	-44.2		
BS353	Parker Hood	32.58	-97.79	270	0.6	<0.002	<0.003	120	-43.1		
BS354	Parker Hood	32.58	-97.77	380	<0.001	<0.002	<0.003	n.a.	b.d.		
BS354A	Parker Hood	32.58	-97.77	380	0.2	<0.002	<0.003	40	-34.8	20.9	0.6
BS355	Parker Hood	32.57	-97.78	225	20.1	2.7	0.1	7	-48.6		
BS355A	Parker Hood	32.57	-97.78	225	12.7	1.8	<0.003	7	-51.3	9.4	0.4
BS356	Parker Hood	32.56	-97.79		1.8	0.1	<0.003	17	-43.1		
BS356A	Parker Hood	32.56	-97.79		1.4	0.1	<0.003	14	-42.9	24.5	0.6
BS357	Parker Hood	32.57	-97.79	240	3.1	0.1	<0.003	30	-46.4		
BS357A	Parker Hood	32.57	-97.79	240	2.1	0.1	<0.003	20	-43.7	19.4	-0.1
BS358	Parker Hood	32.57	-97.78	360	14.6	2.2	0.9	5	-48.2		
BS358A	Parker Hood	32.57	-97.78	360	18	3.5	1.7	3	-41.3		
BS360	Parker Hood	32.58	-97.78	322	1.2	0.1	<0.003	12	-46		
BS361	Parker Hood	32.57	-97.79	210	3.3	0.3	<0.003	11	-48.7		
BS362	Parker Hood	32.56	-97.79	180	4.4	0.3	<0.003	15	-48.5		
BS363	Parker Hood	32.56	-97.79	120	1.3	0.1	<0.003	13	-42.8		
BS369	Parker Hood	32.57	-97.79	300	12.1	1.7	0.2	6	-45		
BS369A	Parker Hood	32.57	-97.79	300	11.9	1.7	0.2	6	-51.4	13.4	0.2
BS434	Parker Hood	32.57	-97.79		6	0.6	<0.003	10	-45.7		
BS434A	Parker Hood	32.57	-97.79		4.8	0.5	0.1	8	-52.4	18.4	0.7
BS435	Parker Hood	32.52	-97.8	180	0.3	<0.002	<0.003	60	-40.9		
BS436	Parker Hood	32.52	-97.76	320	1.1	0.1	<0.003	11	-50.1		
BS443	Parker Hood	32.53	-97.76	420	3.3	0.2	<0.003	16	-50.5		
BS444	Parker Hood	32.53	-97.76	220	3.1	0.1	<0.003	30	-51.4		
BS447	Parker Hood	32.58	-97.77		0.5	<0.002	<0.003	100	-34.6		
BS447A	Parker Hood	32.58	-97.77		0.7	<0.002	<0.003	140	-36.7	20.5	0.5
BS448	Parker Hood	32.58	-97.77		0.8	<0.002	<0.003	160	-35.1		
BS533	Parker Hood	32.54	-97.73	500	9.8	0.9	0.1	10	-51.3		
BS533B	Parker Hood	32.54	-97.73	500	13.4	1	<0.003	13	-52		
BS533C	Parker Hood	32.54	-97.73	500	17	1.6	0.1	10	-45.1	12.3	0
BS544	Parker Hood	32.49	-97.76	420	2.6	<0.002	<0.003	520	-57.4		
BS544A	Parker Hood	32.49	-97.76	420	0.9	<0.002	<0.003	180	-54.1	16.1	0.2
BS551	Parker Hood	32.56	-97.76	363	10.3	1.8	0.3	5	-50	6.7	-0.4
BS552	Parker Hood	32.56	-97.76	385	3	0.4	0.1	6	-51.5		
BS553	Parker Hood	32.56	-97.76		19.4	2.8	0.7	6	-50.2	7.2	-1.1
BS555	Parker Hood	32.49	-97.76	310	22.7	0.4	0.1	45	-50.9	8.2	-2.4
BS237	Somervell	32.31	-97.73	1350	0.6	<0.002	<0.003	120	-50.1	17.6	0.7
BS307	Somervell	32.32	-97.72	425	11.3	0.8	0.2	11	-55.4		
BS402	Somervell	32.32	-97.72	186	1.1	<0.002	<0.003	220	-79.6		
BS403	Somervell	32.33	-97.72	380	2.7	0.1	<0.003	26	-58.1		
BS404	Somervell	32.32	-97.72	370	0.8	0	<0.003	267	-56.4		
BS405	Somervell	32.33	-97.72	500	2.7	0.1	<0.003	26	-59.9		
BS406	Somervell	32.32	-97.72	395	0.9	<0.002	<0.003	180	-57.1		